Coulomb-blockade oscillations in a double quantum dot system

Kemerink, M.

Award date:
1993

Coulomb-Blockade Oscillations in a Double Quantum Dot System

Martijn Kemerink

Afstudeerverslag Technische Universiteit Eindhoven

Eindhoven, september 1993.
Afstudeerhoogleraar (TUE): Prof. Dr. J.H. Wolter.
Begeleider (Philips Nat. Lab.): Dr. L.W. Molenkamp

Abstract

We used a sample consisting of two quantum dots, defined by metalic top gates in a high mobility GaAs-$Al_xGa_{1-x}As$ heterostructure, to study interactions between nearby quantum dots.

We present the first experimental data on stochastic Coulomb blockade. This effect occurs when two dots are placed electricaly in series. We found that its thermal breakdown is linear in T, if $k_BT << e^2/C$, as can qualitatively be understood in terms of thermal smearing of resonance lines.

When in Coulomb blockade, the conductance of a quantum dot is very sensitive to nearby potentials, for example of another quantum dot. We used this to monitor the potential of a quantum dot exhibiting Coulomb blockade oscillations, both in zero and nonzero magnetic field. We found that the dot potential varies in a sawtooth-like fashion for isolated dots (high tunnel barriers). The sawtooth becomes rounded for lower (up to tunnel barriers adjusted to $1½e^2/h$ potential fluctuations were seen) tunnel barriers.

Using a quantum dot as a voltage probe we showed that the strongly modulated conductance signal is fully due to Coulomb blockade and can not be explained by the Ahronov-Bohm effect.

In both experiments we found proof for a resonance line broadening that can not be explained by bulk temperature. For a bulk temperature of 25 mK we found an effective electron temperature of 0.2 K, in agreement with Staring *et al.* [3].

Contents

chapter 1

Introduction

1.1 Preface

Due to the industrial strive for smaller and faster devices during the last decades, a new field of physics is developing, called mesoscopic physics. New physical phenomena have been found in devices with typical dimensions of the same order of magnitude as physically relevant length scales. Examples of such phenomena are quantum interference, ballistic transport and quantum confinement; the corresponding length scales are the quantum phase coherence length, the mean free path and the Fermi wavelength, respectively.
Since these lengths exceed atomical and molecular (microscopical) sizes, and are smaller then macroscopic sizes, one calls them 'mesoscopic'. The devices are commonly called 'nanostructures'.

In figure (1.1) three transport regimes are shown for electrical transport through a wire. In the upper situation, where the electron mean free path l_e is smaller then the typical device dimensions, conventional transport, dominated by impurity scattering, will occur. In the lower figure, where $l_e > W,L$, the transport will be ballistic and will be dominated by the device geometry. This regime is nowadays mainly achieved in semiconductor structures.
Another effect that occurs at these mesoscopic scales is Coulomb blockade: Due to charging effects, transport through a region in which a number of electrons are confined, becomes impossible. In chapter two Coulomb blockade will be discussed in more extent.

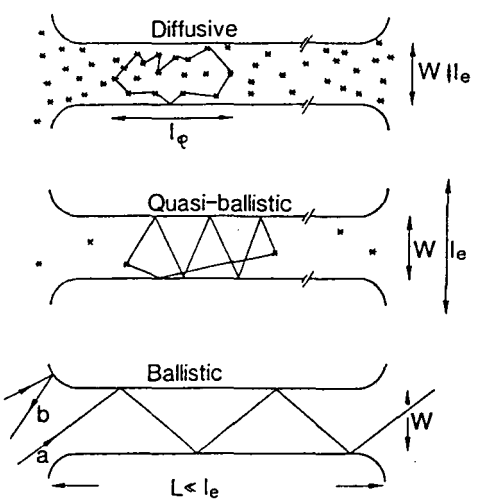

Figure 1.1 Electron trajectories typical for the three transport regimes.

1.2 The two-dimensional electron gas.

In this paragraph a short description of the semiconductor material used in our experiments will be given. The main physical properties of this two dimensional electron gas will also be outlined. In chapter three device structuring and experimental techniques will be described.

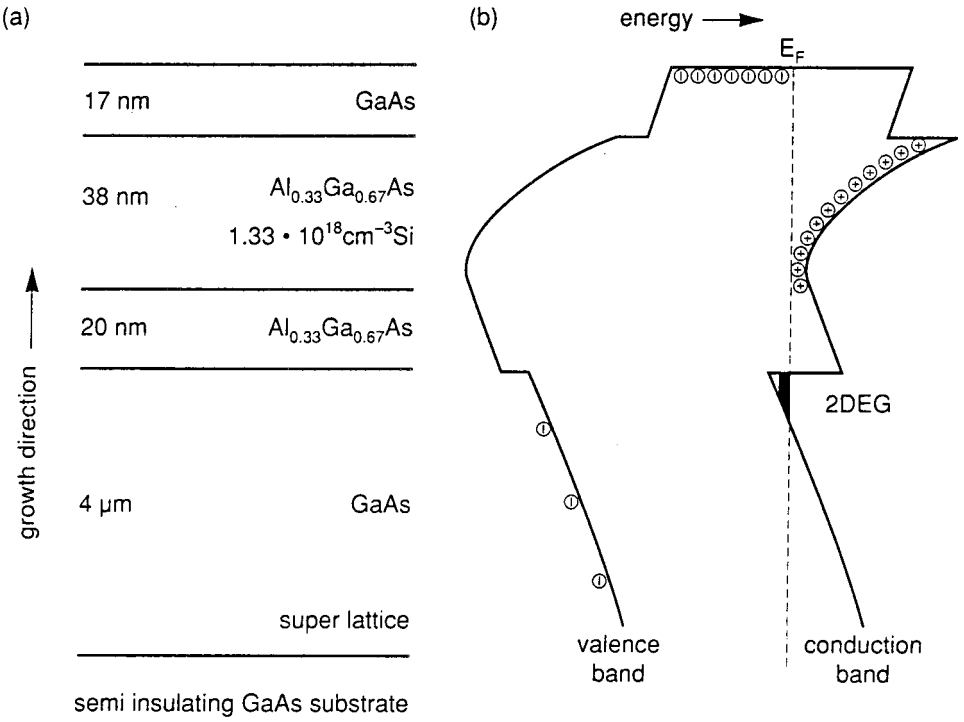

Figure 1.2 Layers of a modulation doped GaAs-Al_xGa_{1-x} heterostructure (a) and the corresponding band-bending diagram (b). The numbers give typical dimensions.

The structures we used are defined by metallic gates on top of an GaAs-$Al_xGa_{1-x}As$ heterostructure. The two-dimensional electron gas (2DEG) is situated in a nearly triangular potential well between the $Al_xGa_{1-x}As$ and the GaAs layers, see figure (1.2).

The heterostructures were grown by Molecular Beam Epitaxy (MBE) at the Philips Research Laboratories, Redhill England by C.T. Foxon and have a typical mobility μ of about $1*10^6$ cm^2/Vs. The typical sheet carrier concentration n is about $1.8*10^{11}$ cm^{-2}, which yields, according to

$$l_e = v_F \tau = \frac{\hbar}{e}(2\pi n)^{\frac{1}{2}}\mu \qquad (1.1)$$

with v_F the Fermi velocity and Y the scattering time, an electron mean free path l_e=7 μm.

As a result of the low electron density the Fermi wavelength is large, in the order of 50 nm. The energy of non-interacting electrons in an unbounded 2DEG is

$$E(k) = \frac{\hbar^2 k^2}{2m} \tag{1.2}$$

which is isotropic as a function of momentum $\hbar k$, parallel to the plane. The effective mass m in GaAs is $m=0.067m_0$.The 2D density of states

$$\rho_{2D} = \frac{m}{\pi\hbar^2} \tag{1.3}$$

is independent of energy, if there is only one occupied subband, which is usually the case. In equilibrium, the states are occupied according to the Fermi-Dirac distribution

$$f(E-E_F) = \left[1+\exp\left(\frac{E-E_F}{k_B T}\right)\right]^{-1} \tag{1.4}$$

When a strong magnetic field B is applied perpendicular to the 2DEG, a discrete energy spectrum arises, since no free motion parallel to B is possible, unlike in bulk GaAs where the energy spectrum exhibits peaks, but does not become fully discrete. In 2D highly degenerated Landau levels are formed at energies

$$E_n = (n-\frac{1}{2})\hbar\omega_c \tag{1.5}$$

where $\Omega_c=eB/m$ is the cyclotron frequency and n an integer. The degeneracy of one Landau level is

$$d = \frac{m\omega_c}{\pi\hbar} \tag{1.6}$$

which is not dependent on the electron density. This yields for the number of occupied Landau levels

$$N_L \approx \frac{E_F}{\hbar\omega_c} \tag{1.7}$$

In the modern theory of the quantum Hall effect, the current carrying states are described as edge states that move along equipotentials of the confining potential V(r), for E_F inbe-

tween two Landau levels, see figure (1.3). Normally one Landau level consists of edge states and localized states, all with quantum number n. The localized states do not contribute to the conductance. These edge states are the quantum mechanical analog of the skipping orbits of electrons undergoing repeated specular reflections at the boundary (confining potential).

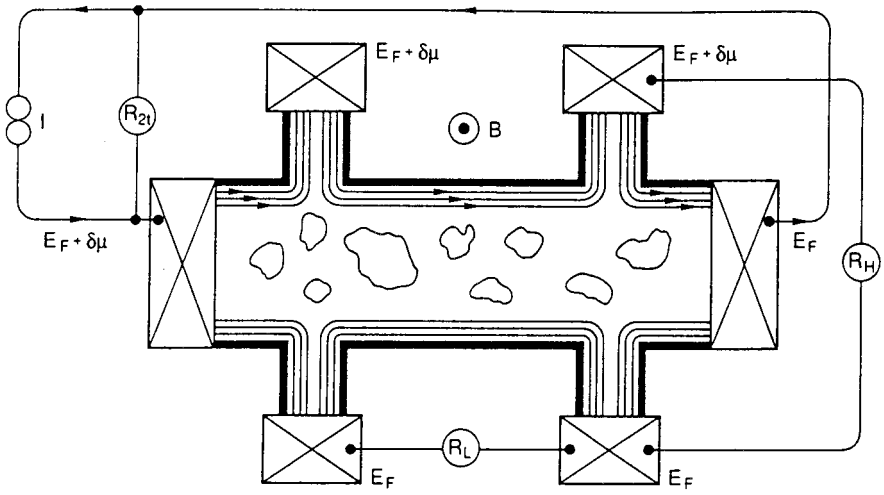

Figure 1.3 Illustration of edge chanels. The arrows point in the direction of motion of the edge states. The localized states do not contribute to the conductance.

Chapter 2

Coulomb blockade oscillations

Since Coulomb blockade is a rather complex phenomena, its description will be done in two steps. In the first paragraph of this chapter a qualitative introduction to Coulomb blockade is given. In paragraph 2.2 a more quantitative treatment is presented.

2.1 Introduction

The first experiment in which Coulomb blockade was observed was the resistance measurement of films of small metallic grains. These films showed a strong increase in resistance at low temperatures, and the explanation given by Gorter [1] in 1951 was that transport through a grain might be inhibited at low temperatures due to charging effects.

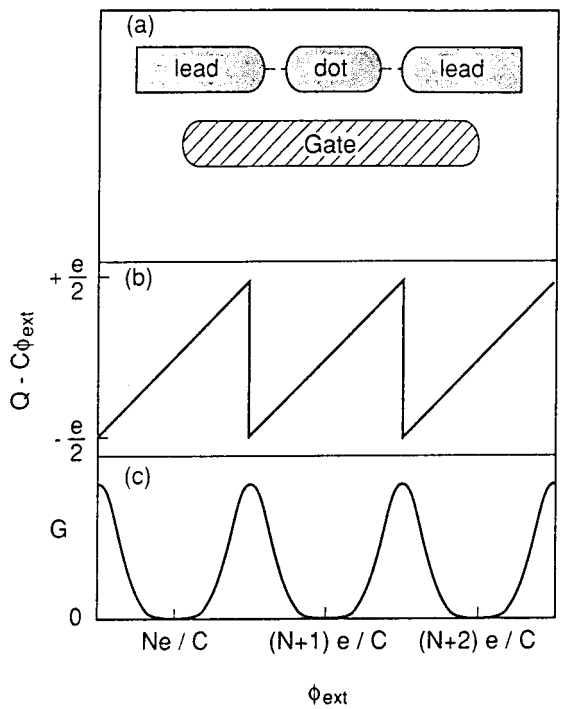

Figure 2.1 (a) Schematic illustration of the system used by Fulton et al. The dashed lines indicate tunnel barriers. (b) The charge imbalance between dot and leads. (c) The periodic conductance of a dot.

Only in 1987, when lithographic technology had come to a sufficiently high level, this hypothesis was verified by an experiment by Fulton et al. [2]. They made a Coulomb blockade transistor, exhibiting periodic oscillations in the conductance as a function of gate voltage.
A schematic lay-out of system used by Fulton et al. is given in figure (2.1). A small metallic island, or dot, is weakly coupled to two conducting leads by tunnel junctions. An additional gate electrode can be used to control the charge on the dot. The charge on the dot is an integer number of conduction electrons, i.e. Q=Ne, with N the number of electrons. Using a fixed number of electrons implies that the dot is coupled very weakly to the leads, by tunnel conductivities much smaller than the conductance quantum e^2/h. When C is the capacitance between dot and nearby charges, for example on the gate, these charges induce a displacement charge $C\phi_{ext}$ on the dot. Minimalisation of the charge imbalance $C\phi_{ext}$-Ne determines N at low temperatures, i.e such that $kT << e^2/C$ with e^2/C the charging energy. In order to fulfil this condition at reachable temperatures, it is necessary to make C typically smaller than 10^{-16}F. Structures with such low capacitances have lithographical dimensions in the order of 1 μm or smaller.
By changing the external potential we can change the charge imbalance on the dot. When, while increasing ϕ_{ext}, the charge imbalance becomes more than e/2, an extra electron is added to the dot, and $C\phi_{ext}$-Ne becomes -e/2. When the condition $kT << e^2/C$ is fulfilled, it is in general impossible to add an extra electron to the dot, and electrical transport through the dot is impossible. Only when ϕ_{ext} is at certain values, (N+1/2)e/C, where the charge imbalance is +/- e/2, there is thermodynamical indifference whether there are N or N+1 electrons on the dot and electrons can tunnel, one by one, through the dot.

In contrast to the experiment described above, our experiments are done on structures defined in semiconductors by use of a split gate technique. When a negative voltage is applied to metallic top gates, the 2DEG underneath is depleted and, for example, a dot, which consists of a few to a few hundreds of electrons, is formed, like in figure (2.2)c. The dot is coupled to the leads by two point contacts, closed beyond the resistance quantum h/e^2, that function as tunnel barriers.

Since the Fermi wavelength is comparable to the dimensions of the dot, the energy spectrum of the electrons may no longer be regarded as a continuum, as we implicitly assumed for metallic dots. Because this size effect becomes important, a dot defined by this means in a 2DEG is often called a 'quantum dot'. In a typical experiment the quantum dot contains $N \approx 100$ electrons and the average energy level spacing is $\Delta E \approx 0.1$ meV, corresponding, via $k_BT=\Delta E$, to a temperature $T \approx 100$ mK. This is the reason most experiments are done in a dilution refrigerator.
Other structures exhibiting Coulomb blockade effects are shown in figures (2.2)a and b.

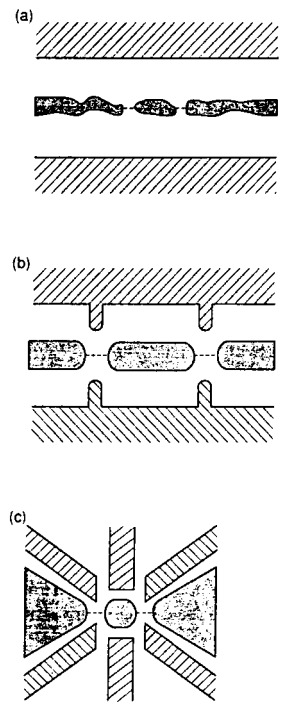

Figure 2.2 Schematic top-view of three semiconductor nanostructures exhibiting Coulomb blockade.

The structure shown in a is called a disordered quantum wire and consists of small conducting islands, separated by depleted regions (tunnel barriers). This occurs when a wire is almost pinched off by applying a large negative bias on the gates. A considerable amount of research has been done on the structures in figure (2.2) during the past few years [3], [4]. Recently, theoretical work on systems consisting of two quantum dots has been done [7], and some experimental results on a lateral double dot structure have been reported [17]. Still, interactions between two nearby quantum dots in a split-gate sample had not been investigated. That will be the main subject of this report.

2.2 periodicity

In this paragraph the periodicity of the conductance of a quantum dot as a function of an external potential will be discussed. Only a short summary of those subjects needed to understand the rest of this report will be given. For a more extensive review of Coulomb blockade, see [5].

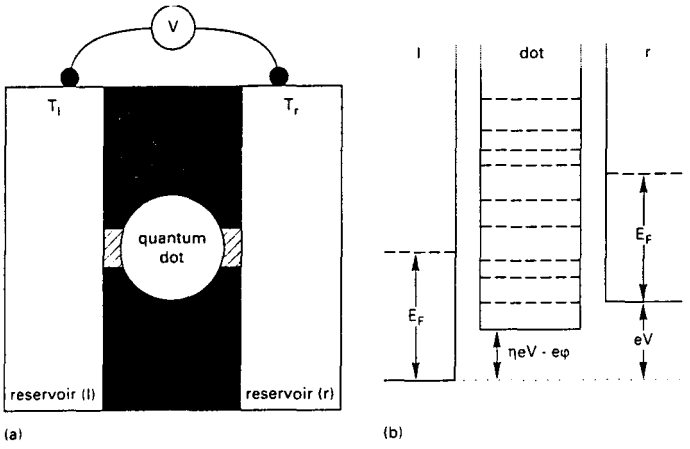

Figure 2.3 (a) Schematic diagram of a quantum dot with tunnel barriers (hatched) and resevoirs. (b) Profile of the electrostatic potential energy (solid line) along a line through the tunnel barriers.

We shall consider a system as shown in figure (2.3). A confined region, the quantum dot, that is weekly coupled by tunnel barriers to two conducting reservoirs. For the sake of simplicity we shall assume that there is no temperature difference across the dot.
When a small voltage difference $V << \Delta E$ is applied between the reservoirs, the conductance G of the dot is

$$G \equiv \frac{I}{V} \tag{2.1}$$

When charging effects are not considered, and $T << \Delta E/k_B$, transport through the dot is only possible if the Fermi levels in the left and right reservoirs line up with an one-electron level in the dot. This process is called resonant tunnelling.

When we do consider charging effects, this condition will be changed. Since the number of electrons on the dot can take on integer values only, a charge imbalance or, equivalently, an excess potential ϕ can arise between the dot and the reservoirs. With Q=Ne the charge on the dot, C the capacitance and ϕ_{ext} the external potential due to e.g. nearby donors or a gate electrode, we can write

$$\phi(Q) = \frac{Q}{C} + \phi_{ext} \tag{2.2}$$

The electrostatic energy U(N) then becomes

$$U(N) = \int_{0}^{-Ne} \phi(Q)\,dQ = \frac{(Ne)^2}{2C} - Ne\phi_{ext} \tag{2.3}$$

In order to make transport through the dot possible, it is necessary that the probability to find a certain number of electrons in the dot, is nonzero for both N and N+1 electrons in the dot. Then, transport is possible by adding one electron from, e.g. , the left and removing it to the right etcetera, so transport takes place via the intermediate states N and N+1. The probability to find N electrons in the dot, in equilibrium with the reservoirs is given by the grand canonical distribution function

$$P(N) = constant \times \exp\left[-\frac{F(N) - NE_F}{k_B T}\right] \tag{2.4}$$

with F(N) the free energy of the dot. This distribution function has an infinitesimal width at T=0 and thus, at T=0, P(N) is generally nonzero for only one value of N, that is the N that minimizes the thermodynamic potential Ω.

$$\Omega(N) \equiv F(N) - NE_F \tag{2.5}$$

Thus, in general the conductance G=0 at T=0. For T unequal to zero the distribution function has a finite width and P(N) can be nonzero for more than one N. For conductance to occur both P(N) and P(N+1) have to be nonzero, and thus N and N+1 have to minimize Ω. A necessary and usually sufficient, unless Ω has more than one minimum, what is usually not the case, condition is $\Omega(N)=\Omega(N+1)$, or

$$F(N+1) - F(N) = E_F \tag{2.6}$$

At T=0 the free energy equals the ground state energy of the dot. This can, simplified, be written as

$$F(N) = U(N) + \sum_{p=1}^{N} E_p \tag{2.7}$$

Together this yields as a condition for a peak in the low-temperature conductance

$$E_N + U(N) - U(N-1) = E_F \tag{2.8}$$

This condition can be fulfilled for any N, so for each N there is a peak in the conductance, yielding a (quasi) periodic conductance spectrum as a function of Fermi energy. By substitution of (2.3) for U(N) this gives

$$E_N^* \equiv E_N + (N - \frac{1}{2})\frac{e^2}{C} = E_F + e\phi_{ext} \tag{2.9}$$

The E_N^* are the renormalized energy levels. The renormalized energy level spacing $\Delta E_N^* = \Delta E + e^2/C$ is enhanced above the normal energy level spacing by the charging energy e^2/C.
The whole process of transport through a dot in the Coulomb blockade regime is summarized in figure (2.4). The energy levels indicated are the renormalized levels.

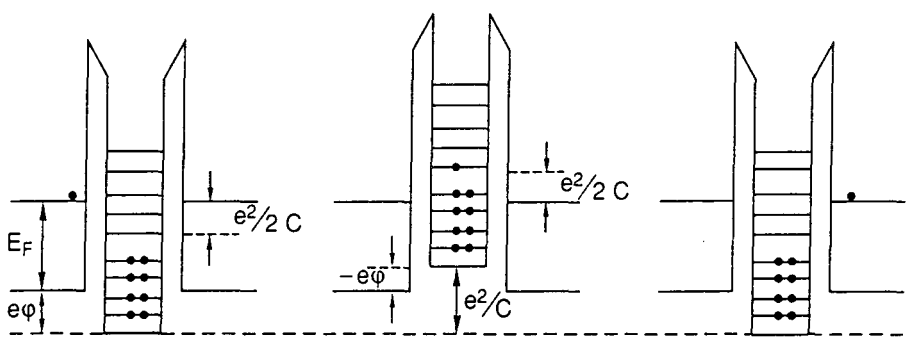

Figure 2.4 Single electron tunneling through a quantum dot. During transport the charge imbalance switches between ±e/2.

Though it is theoretically convenient to vary the Fermi levels in the leads, it is from an experimental point of view interesting to consider a variation in the external potential ϕ_{ext}. The external potential is caused by nearby ionized donors and one or more gate electrodes.

$$\phi_{ext} = \phi_{donors} + \alpha\phi_{gate} \tag{2.10}$$

In figure (2.5) the electrical equivalent of a single quantum dot is shown. It follows

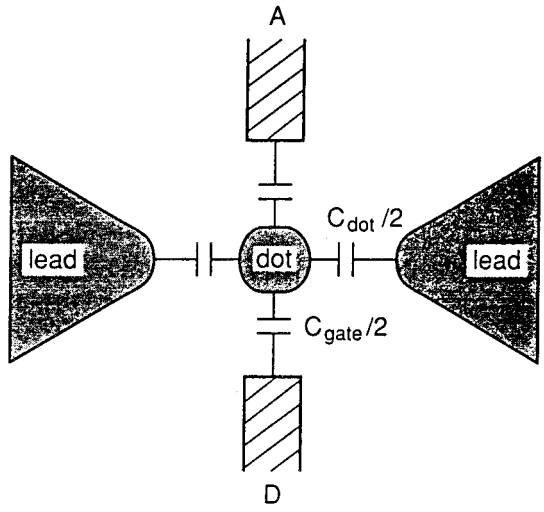

Figure 2.5 Electrical equivalent of a quantum dot with gates (hatched) and leads (shaded). $C=C_{dot}+C_{gate}$.

simply that $\alpha=C_{gate}/C$ with $C=C_{gate}+C_{dot}$. When combined with (2.9) this yields for the periodicity in the external gate potential

$$\Delta\phi_{gate} = \frac{e}{C_{gate}}\left[1+\frac{\Delta E_N}{e^2/C}\right] \tag{2.11}$$

In our experiments e^2/C is about 5 times bigger than ΔE_N. Only for simplicity we shall mostly neglect the second term in (2.11), and assume $\Delta\phi_{gate}=e/C_{gate}$. When we take $\phi_{gate}=V_{gate}$, what is allowed for a dot with wide leads, we find

$$\Delta V_{gate} = \frac{e}{C_{gate}} \tag{2.12}$$

Not only the conductance of a quantum dot oscillates as a function of gate voltage, also the potential of the dot, relative to the lead potential, oscillates with V_{gate}. In figure (2.1)b the charge imbalance as a function of ϕ_{ext} is shown to oscillate between +e/2 and -e/2 in a sawtooth-like way. Because V=Q/C for a capacitive system, we find that the relative potential of the dot varies between +e/2C and -e/2C in the same sawtooth-like fashion; Increasing linearly with increasing V_{gate} and dropping discontinuously when it is energetically favourable to add an extra electron.

chapter 3

Experimental

The samples used in our experiments were all made out of one piece of $Al_xGa_{1-x}As$-GaAs material (wafer G868D) with a typical mobility of $1*10^6$ cm^2/Vs and an electron density of $1.8*10^{11}$ cm^{-2}.

3.1 Split gate technique and sample production

The electron gas is shaped by two techniques: (wet) mesa-etching, resulting in a permanent removal of the electron gas, and electrostatic depletion by applying a negative bias to metallic gates on top of the sample, see figure (3.1).

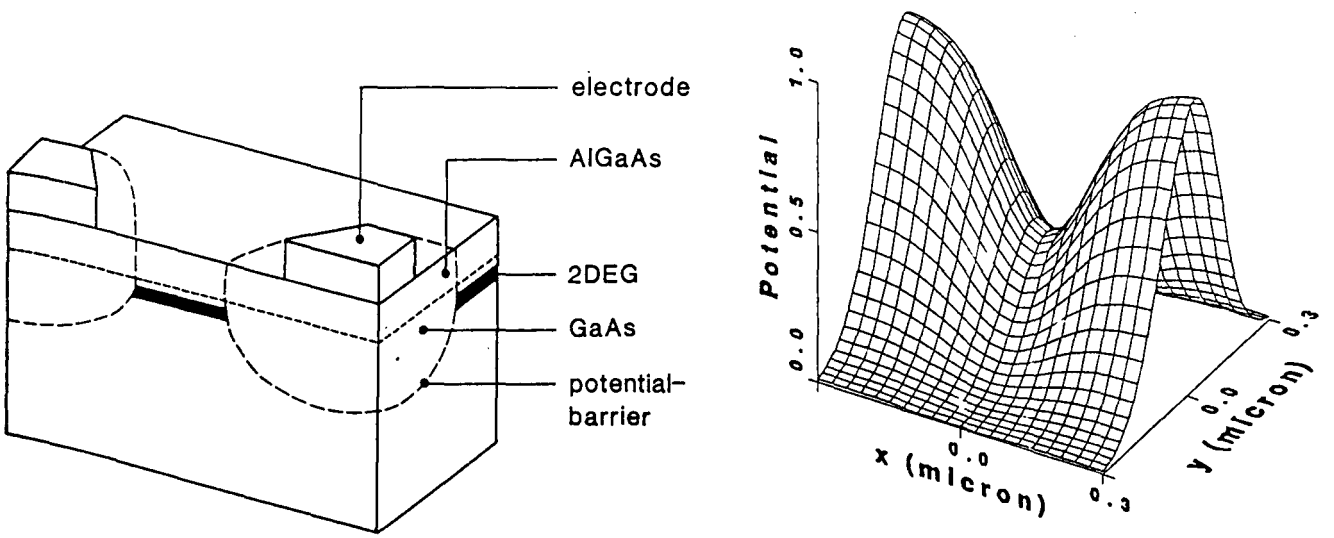

Figure 3.1 A heterostructure with a metalic top gate on top. The electrons in the 2-DEG are depleted by a smooth potential barrier.

The advantage of this split gate technique is that the depletion width is a smooth function of the gate voltage and thereafter constrictions with a variable width can be made, like point contacts and (disordered) quantum wires. It, too, gives the opportunity to regulate, to a certain extent, the number of electrons in a quantum dot and thereby changing the coupling to nearby potentials, e.g. on gates or of another dot.

The first step in the production of a sample is the mesa etching of a 1*0.3 mm Hall bar on top of the heterostructure. Ohmic contacts are made by alloying Au-Ge-Ni into the 2DEG at the edges of the Hall bar. Then the coarse parts of the Ti-Au gates are structured using a conventional optical lithography. The next step consists of the deposition of bonding pads on the ohmic contacts and on the far ends of gates.
In the last lithographical step the fine parts of the (nano) structure are made using electron beam lithography. The lithographic opening between the split gates defining a tunnel barrier is typically 250 nm.
The last step is separating the samples from another and bonding them to a socket that can be installed in a cryostat.

3.2 The double dot sample

In order to gain better insight in electrical transport through arrays of dots and disordered quantum wires, a sample was designed that made it possible to study the interactions between two nearby dots, see figure (3.2).

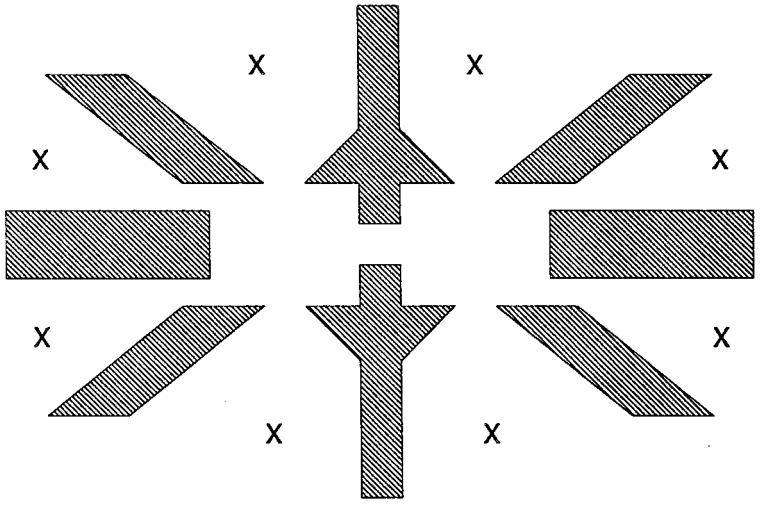

Figure 3.2 Schematic lay-out of the double dot sample. The hatched arreas are metalic top gates, the crosses denote Ohmic contacts.

It consists of two dots separated by a split-gate defined tunnel barrier, which gives the opportunity to use the sample in the full range between one large dot and two completely separated dots. Both separate dots can be measured independently of eachother.

3.3 Measurement techniques

All measurements were performed in a Oxford Instruments dilution refrigerator with a base temperature of 20 mK. Unless stated otherwise, all experiments were done at this temperature. Magnetic fields up to 10 T could be generated using a built-in superconducting magnet and an Oxford Instruments 2127 power supply. The whole setup, including the measurement control computer was installed in a Faraday cage. 220 V AC power supply was generated by a separated generator.
All measurement control was done through a GPIB-interface using 'Asystant' software on a HP Vectra ES/12 computer. Constant gate voltages were generated by a Keithley 230 programmable voltage source and a four-channel HP6626A power supply. Gatescans were made using a HP 3245A universal source.

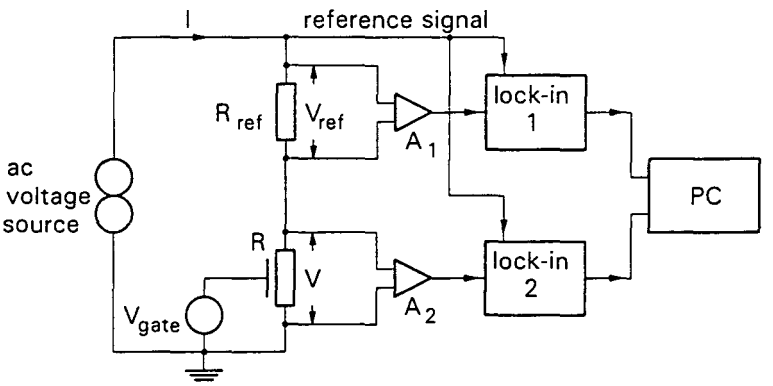

Figure 3.3 Schematic diagram of the measurement circuit. Only the device is at low temperature. The whole setup is surraounded by a Faraday cage.

A standard low frequency ac double lock-in method was used for most measurements. In figure (3.3) the system is schematically shown. A Philips PM 5168 function generator and a PM 5180 attenuator supplied the 10 μV, 10 Hz driving voltage. An EG&G Princeton Applied Research model 5204 and a Ortholoc model 9502 lock-in amplifier were used for the detection of the sample and reference signals, respectively.

chapter 4

Stochastic Coulomb blockade

This far, we considered the conductance of a single quantum dot as a function of gate voltage. The situation becomes qualitatively different when a number of dots is placed in series, like in a disordered quantum wire with multiple conductance limiting elements. Here, we shall study the most simple case with two dots in series. In our double-dot device this means that the central tunnel barrier is adjusted at $G \approx 1/4\ e^2/h$ so two weakly connected dots are formed. Other tunnel barriers are also adjusted at $1/4\ e^2/h$ if needed for conductance and closed otherwise.
For a more extended review of the stochastic Coulomb blockade theory in paragraph 4.1 see [6], [7].

4.1 Introduction

In chapter 2 we found as a condition for nonzero conductivity of a quantum dot

$$V_{gate} = \frac{e}{C_{gate}}(N + \frac{1}{2}), \quad N = 0, \pm 1, \pm 2, ... \tag{4.1}$$

where C_0 is the dot-to-gate capacitance. This is true for temperatures that are low compared to the renormalized energy levels E_N^*.

$$k_B T \ll \frac{e^2}{2(C_{gate} + C_{dot})} \tag{4.2}$$

Hereby we assumed that ϕ_{gate} and V_{gate} are the same, which is allowed for a quantum dot with wide leads. Further, we neglected the one electron energy level spacing.
When two dots are placed in series, two conditions for V_{gate} have to be fulfilled. The electrical equivalent of such a system is given in figure (4.1).

If the dots are not identical the conditions for conductance cannot be fulfilled at the same time at T=0. For finite temperatures, but $k_B T << \Delta E_N^{*1,2}$, the conductance,too, is zero in general. The first question to be answered is when such a system does have a nonzero conductance as a function of gate voltage.

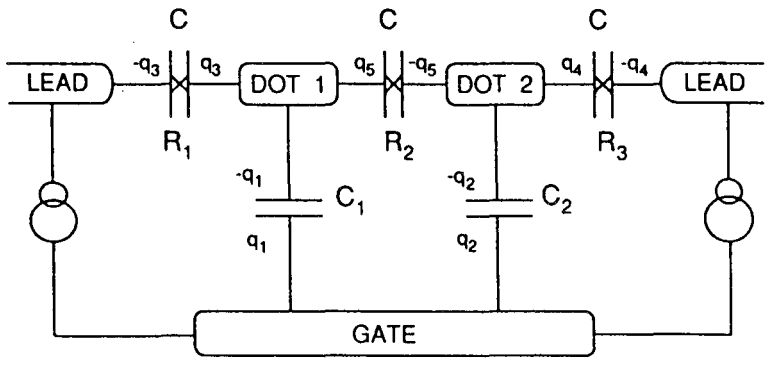

Figure 4.1 Equivalent circuit of a double dot device. The polarisation charges q_i are continuous ones. The charges on the dots $eN_{1,2}$ (not shown) are discrete.

Like in the case of a single dot, we will write down an expression for the electrostatic energy $U(N_1,N_2,V_{gate})$, with $N_{1,2}$ the number of electrons on a dot, and demand that for both dots there should be energetical indifference between N_i and N_i+1 to make transport through the dot possible.
Using the semi-classical capacitance model of figure (4.1), the electrostatic energy U can be expressed in terms of the polarisation charges $q_1,\ldots,q_5$, and the gate potential V_{gate}.

$$U(q_1,\ldots,q_5) = \frac{q_1^2}{2C_1} + \frac{q_2^2}{2C_2} + \frac{q_3^2+q_4^2+q_5^2}{2C} + V_{gate}(q_1+q_2) \qquad (4.3)$$

using the shorthand notation C_1, C_2 for $C_{gate,1}$, $C_{gate,2}$ and $C=1/3C_{dot}$. Since N_1 and N_2 are integers, the dot can only contain an integer number of electrons, this implies for $q_1,\ldots,q_5$

$$\begin{aligned} q_3+q_5-q_1 &= -N_1e \\ q_4+q_2-q_5 &= -N_2e \end{aligned} \qquad (4.4)$$

The equilibrium charges q_i, at given N_1, N_2, are found from (4.4) and the condition that U is at a minimum, or

$$\frac{\partial U}{\partial q_i} = 0, \quad i = 3,4,5. \qquad (4.5)$$

Straigthforward mathematics gives U as function of the discrete variables N_1, N_2, and the continuous variable V_{gate}.

$$U(N_1,N_2,V_{gate}) = U_{11}N_1^2 + U_{22}N_2^2 + U_{12}N_1N_2 - eV_{gate}(a_1N_1 + a_2N_2) \qquad (4.6)$$

With coefficients

$$U_{ij} = \frac{e^2(2C + c_i\delta_{i,j})}{2(3C^2 + 2CC_1 + 2CC_2 + C_1C_2)}$$
$$a_i = \frac{CC_1 + CC_2 + C_1C_2 + CC_i}{3C^2 + 2CC_1 + 2CC_2 + C_1C_2} \qquad (4.7)$$

These formulas can be simplified by assuming that the dot-to-gate capacitance is much bigger than the dot-to-dot and dot-to-lead capacitance, or

$$C \ll C_1, C_2 . \qquad (4.8)$$

Applying this assumption to (4.7) and (4.6) leads, in zero order approximation, to

$$U(N_1, N_2, V_{gate}) = \frac{\Delta_1 N_1^2}{2} + \frac{\Delta_2 N_2^2}{2} - eV_{gate}(N_1 + N_2)$$
$$\Delta_1 \equiv \frac{e^2}{C_1} \ , \ \Delta_2 \equiv \frac{e^2}{C_2} \qquad (4.9)$$

At low temperatures, the system favours certain N_1, N_2, and, like in the case of a single dot system, transport is only possible if the system is charge degenerate for both dots. This gives two conditions on one parameter, V_{gate}.

$$|U(N_1, N_2) - U(N_1 + 1, N_2)| \le k_B T$$
$$|U(N_1, N_2 + 1) - U(N_1, N_2)| \le k_B T \qquad (4.10)$$

By inserting (4.9) this can be rewritten to

$$|eV_{gate} - (N_1 + \frac{1}{2})\Delta_1| \le k_B T$$
$$|eV_{gate} - (N_2 + \frac{1}{2})\Delta_2| \le k_B T \qquad (4.11)$$

These conditions are illustrated in figure (4.2).

At high temperatures these conditions are easily satisfied for all V_{gate}. At low temperatures, figure (4.2)b ($k_BT << \Delta_1, \Delta_2$), this is generally not the case, and, if C_1/C_2 is an irrational number, only a few conductance peaks will survive both conditions. This gives rise to a conductance spectrum with sparse and irregularly spaced conductance peaks. This is illustrated in figure (4.3), top line. The quasi random spacing is the reason for the, in fact misplaced, name stochastic Coulomb blockade.

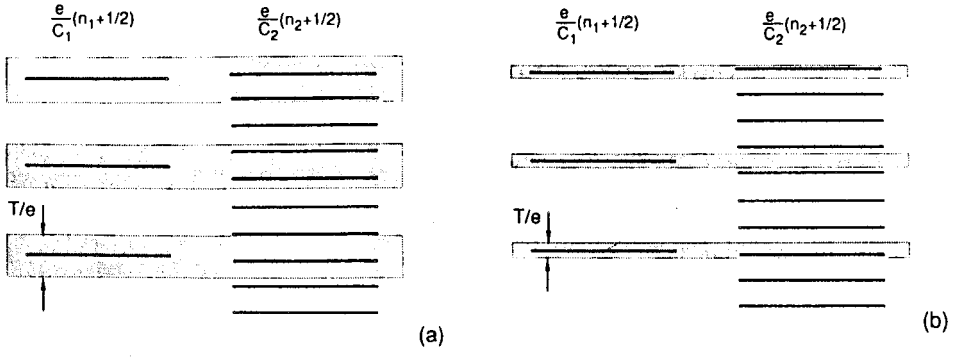

Figure 4.2 The ladder of V_{gate} values favoring transport through the dots. When two rungs of different ladders belong to the same 'thermal' strip, charge easily passes through the system.

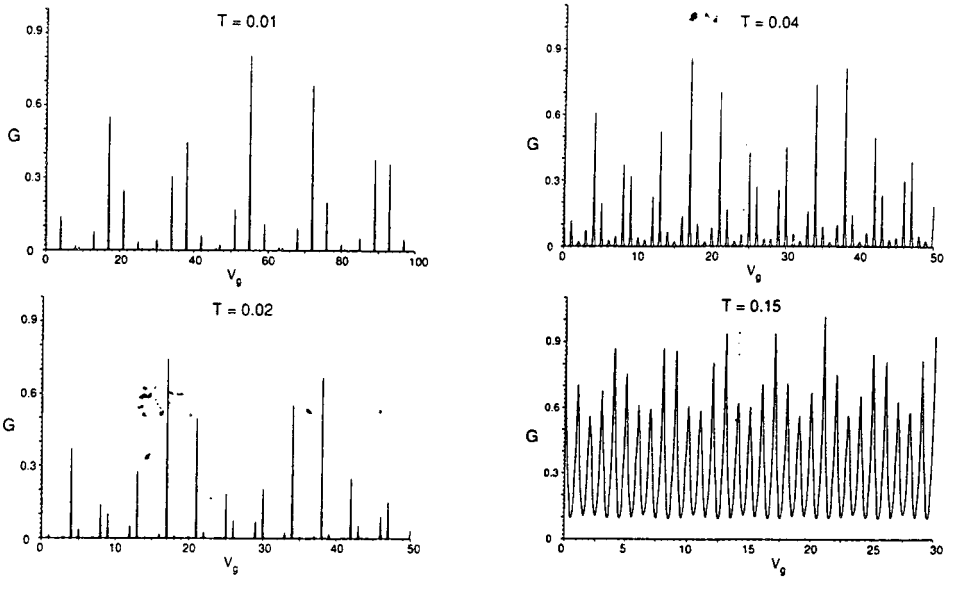

Figure 4.3 Calculated conductance spectrum at 4 different temperatures. V_g and T are measured in units of e/C_1 and e^2/C_2k_B, respectively. $C_1/C_2 \approx 0.36$.

For very different C_1, C_2 and intermediate temperatures

$$\frac{\Delta_2}{2} \leq T \ll \frac{\Delta_1}{2} \tag{4.12}$$

the system behaves as if the larger second dot is replaced by a wide lead, that is as if it has a continuous energy spectrum. See figure (4.2)b and (4.3), lower line. So for very different C_1 and C_2 it is possible to observe both stochastic and regular Coulomb blockade behaviour in the same sample at different temperatures. Numerical simulations by Ruzin *et al.* [7] show that it suffices to have C_1 and C_2 different by a factor two.

Until now we assumed that the dot-to-dot capacitance is larger than the dot-to-lead capacitance, condition (4.8). In our experiments however, this is not true. Generally, $\alpha = C_{gate}/(C_{gate}+C_{dot})$ is about 0.25. This does not really change the physics of the problem, as can be seen from figure (4.4).

4.2 Thermal breakdown

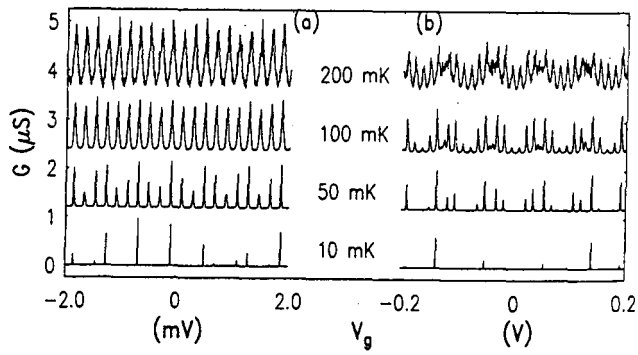

Figure 4.4 Numerical simulation of the conductance of a double dot device with C«C_1,C_2 (a) and C»C_1,C_2 (b).

As was concluded in the preceding paragraph, the number of conductance peeks surviving conditions (4.11) increases with increasing temperature. This is called the thermal breakdown of the stochastic Coulomb blockade. How the number of surviving peeks depends on temperature can be understood from figure (4.5).
Starting from (2.9) we can write for the renormalized energy levels of a double dot system

$$E^*_{N,1} = E_F + e\phi_{ext}$$
$$E^*_{N,2} = E_F + e\phi_{ext} \qquad (4.13)$$

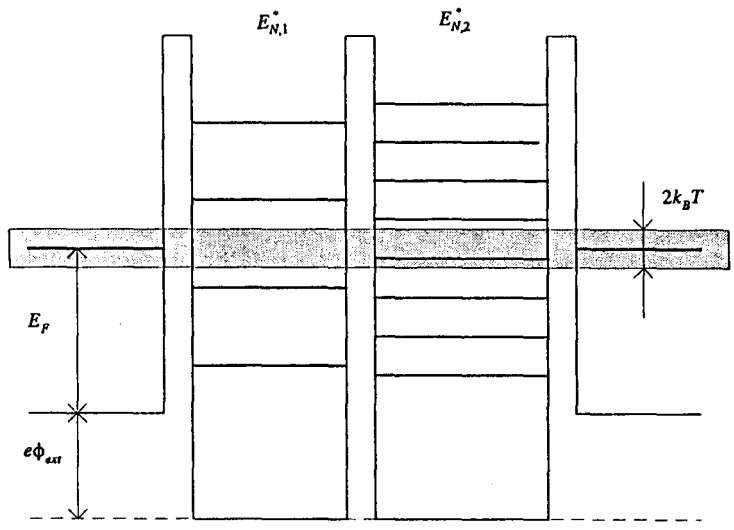

Figure 4.5 Thermal breakdown of stochastical Coulomb blockade. The probability that both energy laders line up, within k_BT, with the Fermi level in the leads, increases lineary with T.

This means that at T=0 both renormalized energy levels should line up with the Fermi level in the reservoirs to make the conductance nonzero. For finite temperatures both E^*_N have to lay, in first order approximation, within k_BT of the Fermi level for G≠0. This is

only true for $T < \Delta E^*_{N,1,2}$. So for small T the number of conductance peaks in a certain interval of the gate voltage should increase linearly with T.

4.3 results

By scanning one gate at a time, C_1 and C_2 were measured and were found to be $2.4*10^{-17}$ and $4.3*10^{-17}$ F, respectively. This yields a ratio $C_2/C_1=1.8$, which proved to be sufficient to observe both stochastic and regular Coulomb blockade oscillations at different temperatures. In figure (4.6) the conductance G of the two dots in series as a function of gate voltage is shown for three different temperatures.

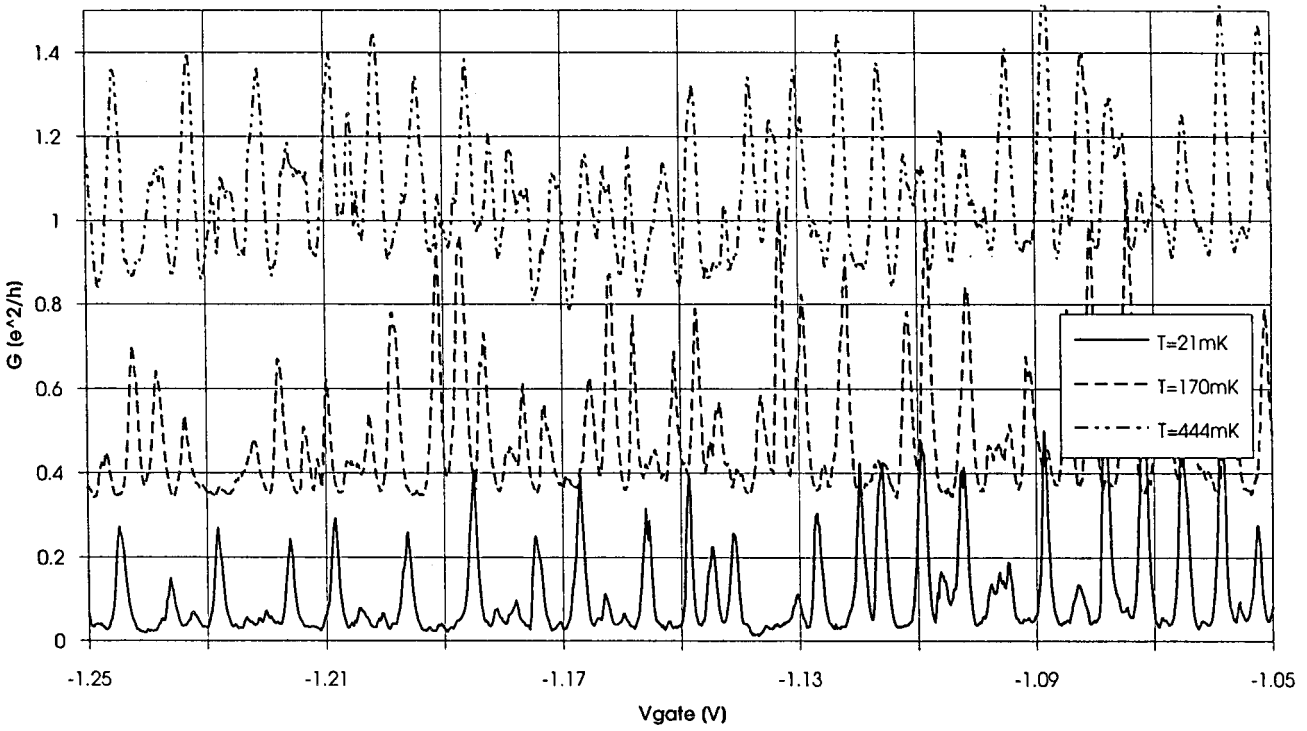

Figure 4.6 Conductance spectrum of two dots in series at three temperatures. The traces are offset for clarity (0, 0.3 and 0.6 e^2/h).

At low temperatures most conductance peaks are suppressed, as can be seen in the figure. Clearly visible is that the non-suppressed conductance peeks are not spaced stochastically, but in a more or less regular way. This beating-like behaviour is what is to be expected, considering the origin of stochastical Coulomb blockade and the fact that the ratio C_2/C_1 is only 1.8.

The 170 mK trace shows a spectrum with about the same periodicity as the 20 mK trace, but with less suppressed peaks.

At high temperatures (444 mK), only a small effect of the conductance oscillations of the bigger dot (dot 2) is visible, as a minor perturbation of the slow oscillations of the smaller dot.

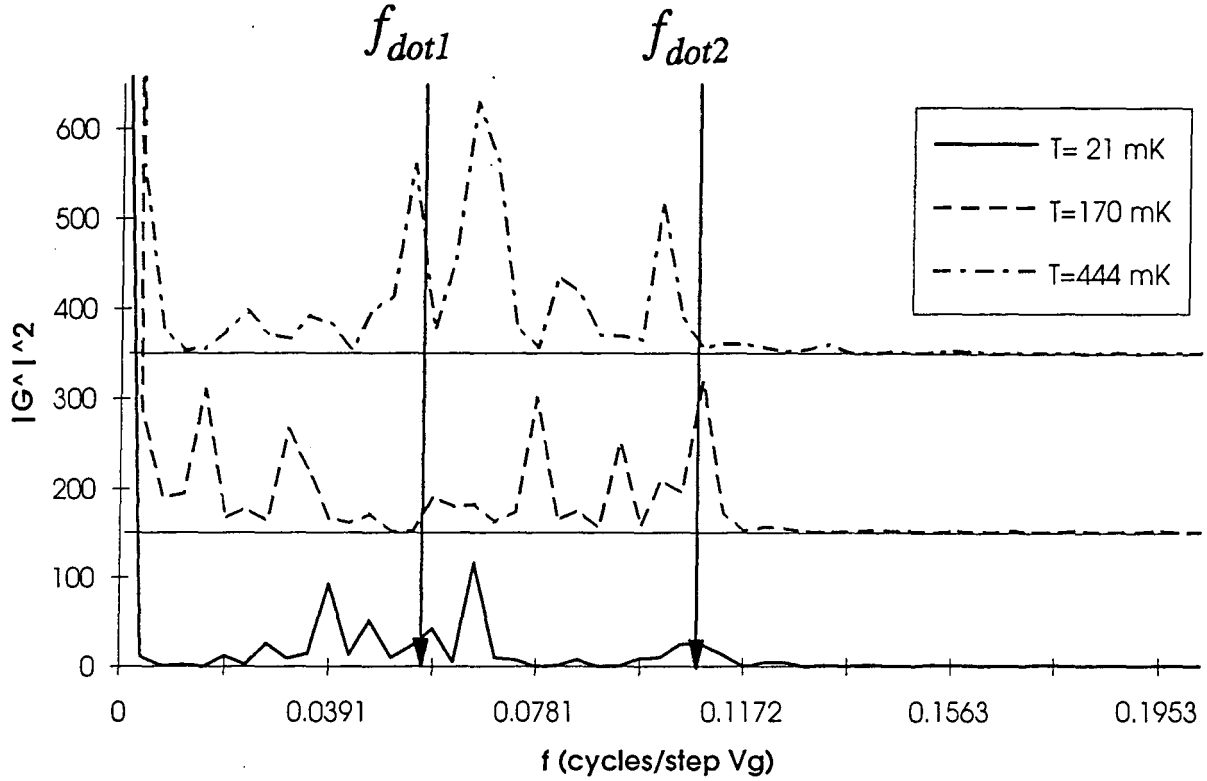

Figure 4.7 Power spectrum of the traces in figure 4.6. The arrows indicate the oscillation frequencies of the separate dots.

This picture is confirmed by the Fourier spectrum of these traces, see figure (4.7). The conductance signal at 20 mK has its Fourier maximum clearly at f_{dot1}, what is to be expected since the low-temperature conductance is dominated by the dot that puts the heaviest constriction on the conductance. Since $C_1 < C_2$ and therefore $\Delta E^*_{N,1} > \Delta E^*_{N,2}$, dot 1 has the largest energy level spacing with respect to k_BT and dominates the conductance. The 444 mK Fourier transformed conductance shows that the energy level spectrum of dot 2 is not completely thermally smeared, and may thus not be regarded as continuous, at this temperature because a relatively high, but narrow, peak at f_{dot2} is still visible. This corresponds to the perturbation of the dominating conductance of dot 1 by dot 2. The dominance of dot 1 is visible in the broad and high peaks around f_{dot1}.

A striking feature of the 20 mK conductance trace is the large number of surviving conductance peaks. Because $e^2/Ck_B \approx 4$ K, one would, considering figures (4.3) and (4.4), expect a much smaller number of peaks to be visible. This might be caused by a broadening of the energy levels due to electron-gas heating as a result of residual electrical noise [3] or an intrinsic broadening of the single electron levels. In chapter 5 we will discuss this issue in greater extent.

In the preceding paragraph we saw that the number of conductance peaks that is visible in a certain interval of V_{gate} should increase linearly with T. For sixteen temperatures, ranging from 20 to 500 mK, we made gatescans and counted peaks.

The peakcounting was done by computer (In Appendix A the Pascal program is listed). Before counting started, all conductance scans were background corrected, and normalized on a fixed, for all temperatures equal, maximum conductance

$$G_{norm} = \frac{1}{G_{\max}^{fixed}}(G_{experimental} - G_{background}) \qquad (4.14)$$

The peakcounting program detects peaks that exceed a certain level, in the range from 0 to 1. The results of counting with a detection level of 0.6, giving the clearest results, are shown in figure (4.8).

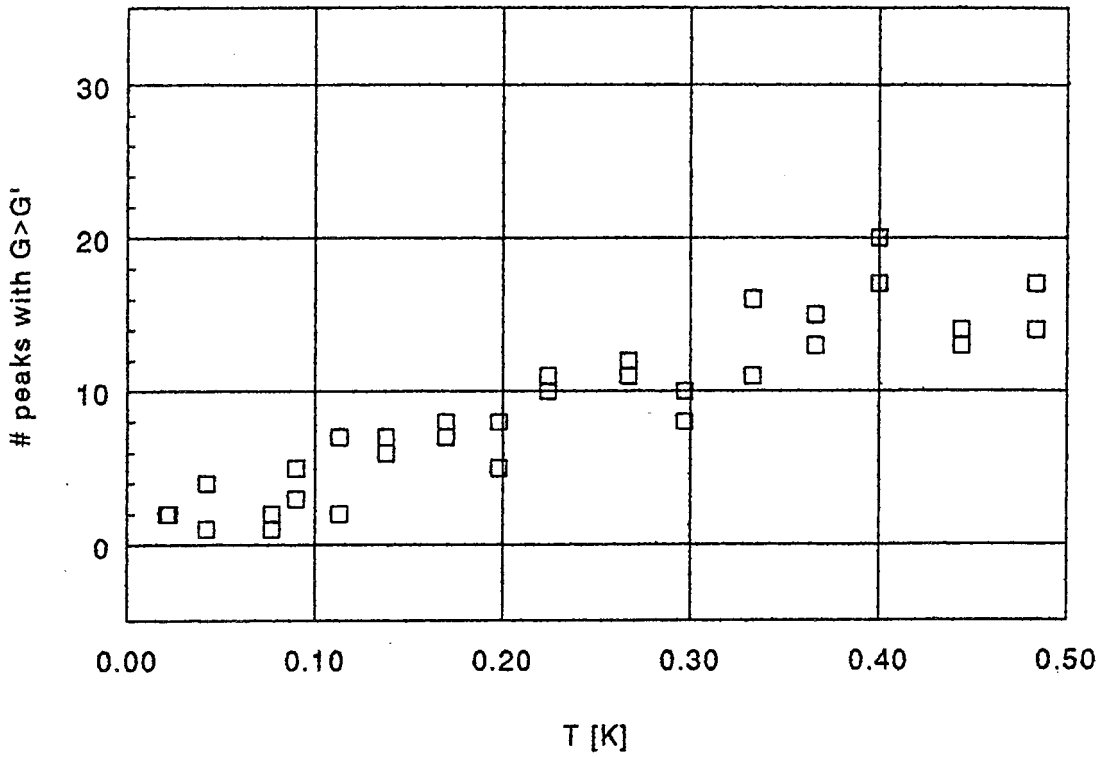

Figure 4.8 Number of measured conductance peaks in a fixed interval of V_{gate}. Only peaks higher than $0.6*G_{max}$ (after background correction) were counted.

The general feature of the figure is a linear increase of the number of detected peaks with T. Only for T>400 mK a saturation is visible, so one could conclude that 0.4 K is the temperature at which the bigger dot becomes unimportant, meaning that the energy level spacing is in de same order of magnitude as $2k_BT$ (and not k_BT, since a dot becomes unimportant when there is always a resonance level within k_BT of the Fermi level, what is the case if the energy level spacing is $2k_BT$). This yields via $\Delta E=e^2/C$ a total capacitance C of $2*10^{-15}$F. Since the Fourier spectrum at 444 mK still shows a clear peak at f_{dot2}, we can estimate that the energy level spacing exceeds the thermal energy at this temperature by a factor two or more. Staring *et al.* [3] found in a similar, single, dot a charging energy of about 1.5 K. Applying this to our system, that has slightly smaller dots, we find $C\approx 5*10^{-16}$ F. This still is a factor three bigger then can be expected from conventional capacitance measurements ($C_1\approx 3*10^{-17}$F and $\alpha\approx 0.2$ yield $C\approx 1.5*10^{-16}$F, $\alpha=0.2$ is

reasonable from a geometrical point of view, since the gate is approxemately ¼ of the border of the dot, so $\alpha = C_{gate}/C_{dot}$ should be in the same order of magnitude) Maybe this effect too is a result of some intrinsic line broadening.

4.4 Conclusion

In this chapter we presented the first experimental data on stochastical Coulomb blockade, and studied its thermal breakdown. We showed that the ratio of gate-to-dot capacities $C_2/C_1 = 1.8$ suffices to observe both stochastical and regular Coulomb blockade behaviour in the same sample at different temperatures.
With the aid of Fourier transforms the dominance at all temperatures of the dot with the largest energy level spacing was shown.
The number of conductance peaks that survives both conditions on V_{gate} increases linearly with T, for small T, as can be expected from a simple thermal smearing model.
In order to understand the exact number of surviving conductance peaks, further study to the resonance line width is needed, since far more conductance peaks survive than can be expected from other experimental data. Furthermore, the biggest dot seems to become unimportant at a temperature that is about a factor three smaller than can be understood from the energy level spacing. These effects may imply that the resonance levels in a quantum dot are broadened in some way, as has been reported before [3]. As stated in the preceding paragraph, this broadening might be caused by electron-gas heating due to electric noise or an intrinsic finite level line width, see also chapter 5.

chapter 5

A quantum dot as voltage probe

In chapter two we saw that the conductance of a quantum dot is strongly dependent on nearby potentials, for example on a metallic gate. In the experiments described in this chapter we will use this sensitivity to nearby potentials to monitor the potential of a dot on the conductance of another dot.

5.1 Introduction

When the first measurements of oscillative behaviour of the conductance of a single quantum dot were reported, there were two main explanations: The Coulomb blockade theory, by Likharev and coworkers [5], as presented in chapter two, and the resonant tunnelling theory [14]. The latter theory claims that charging effects are unimportant and that transport through a dot is possible when the Fermi levels in the leads line up with a single electron level in the dot. The conductance oscillations can then be explained as being caused by the 'scanning' of these levels by the lifting of the energy band bottom due to a potential on a nearby gate. Though the Coulomb blockade theory is nowadays generally accepted as correct, the ultimate prove can be given by measuring the potential of the quantum dot as a function of gate voltage. Unlike the resonant tunnelling theory, the Coulomb blockade theory predicts that the potential of a dot should vary in a sawtooth-like way as a function of gate voltage. See chapter 2.2 and figure (2.1). To measure this potential has been a hard experimental nut, since the voltage probe should be non-invasive, in order not to disturb the dot, and extremely sensitive. Recently, independently of our experiment in which we use a quantum dot as voltage probe, Field et al. [8] used a point contact as a voltage probe.

During the experiments described in this chapter we closed the central tunnel barrier in order to achieve a purely capacitive coupling between both dots. The other tunnel barriers were adjusted to $G \approx 1/4\ e^2/h$, so the conductances of both dots could be measured independently. In figure (5.1) the equivalent electrical circuit of this setup is shown.

From here we shall assume that dot 2 is used as a voltage probe for the potential on dot 1. Only one gate, gate 1, is scanned, the other gates are kept at a constant voltage.
In the following section we will discuss the potentials of both dots, V_{dot1} and V_{dot2}, as a function of gate voltage V_{gate1}. We shall only consider small perturbations on the equilibrium situation, and thereafter we shall use first-order terms in our calculations only.

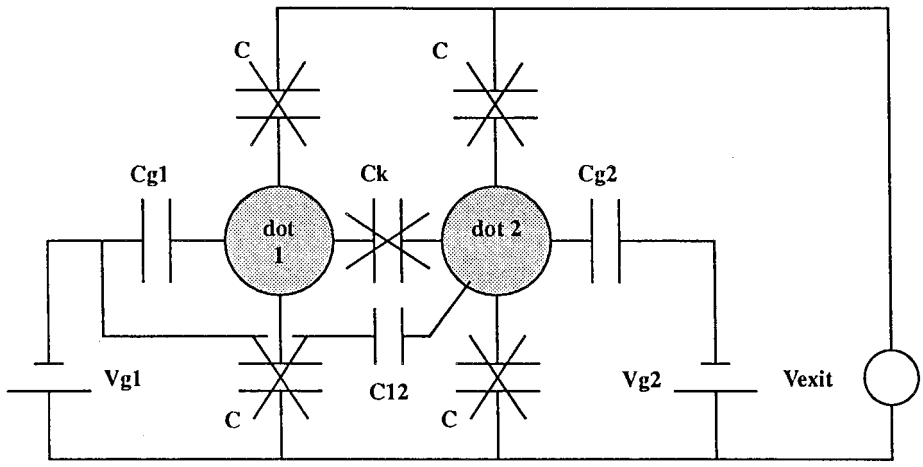

Figure 5.1 Electrical equivalent of the double dot sample, used to model the use of a quantum dot (dot 2) as a voltage probe for the electrostatical potential of dot 1.

Starting with the first dot, we find that a small change of gate potential ΔV_{g1}, induces a perturbation charge on the dot Δq_1

$$\Delta q_1 = C_{g1}\Delta V_{g1} + e\Delta N_1 \tag{5.1}$$

ΔN is included because ΔV_{g1} can cause a change in the number of electrons on the dot. With $\Delta V_{dot1} = \Delta q_1 / C_1$ this yields for the change in potential of dot 1

$$\Delta V_{dot1} = \frac{C_{g1}}{C_1}\Delta V_{g1} + \frac{e}{C_1}\Delta N_1 \tag{5.2}$$

where $C_1 = C_{g1} + C_k + 2C$ is the total capacitance of dot 1. These two terms account for the sawtooth-like oscillations of the potential in the dot, see figure (5.2), top panel.

The second dot is coupled to V_{g1} in two ways; directly via C_{12}, that accounts for the capacitive coupling between gate 1 and dot 2, and indirectly via dot 1 and C_k. In an analog way as for the first dot, we can derive for the potential of dot 2

$$\Delta V_{dot2} = \frac{C_{12}}{C_2}\Delta V_{g1} + \frac{C_k}{C_2}\left(\frac{C_{g1}}{C_1}\Delta V_{g1} + \frac{e}{C_1}\Delta N_1\right) \tag{5.3}$$

In figure (5.2), second panel, ΔV_{dot1} is plotted as a function of V_{g1}. The first term on the right is linearly increasing upon increasing V_{g1}, the second and third term form the oscillating part.

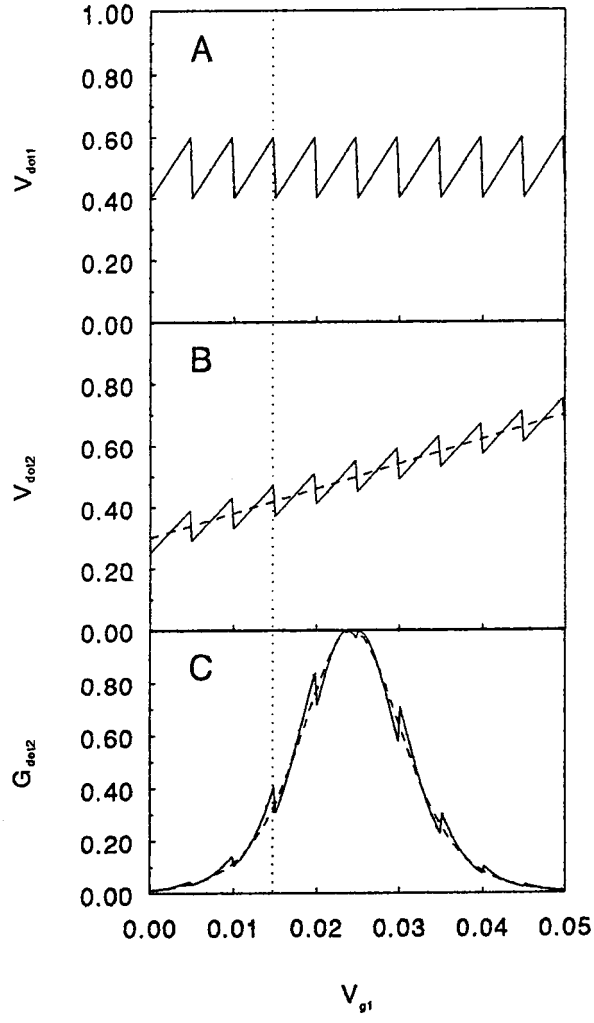

Figure 5.2 Electrostatical potential of dot 1 (a) and 2 (b) and the resulting conductance of dot 2 (c). Dashed lines indicate the situation if dot 1 is not defined, the dotted line guides the eye.

The conductance of the second dot can be computed using [13]

$$\frac{G}{G_{\max}} \approx \cosh^{-2}\left(a\frac{V_{dot2}}{k_B T}\right) \tag{5.4}$$

with a a constant. In appendix A a computer program is discussed that calculates G_{dot2} as a function of V_{g1} with given capacitances and temperature.
Qualitatively the shape of one conductance oscillation of dot 2 can be understood as follows. Due to the coupling between both dots, the sawtooth-like potential of dot 1 (figure (5.2),a) is superimposed on the potential of dot 2 (panel b). Starting at the far left in figure (5.2)b (V_{g1}=0 V), this means that the potential of dot 2 increases stronger, due to charging of dot 1, as V_{g1} is increased, with dot 1 'present' (solid curve) as with dot 1 'not present' (dashed curve). This means that, on the left-hand side of the figure, the conductance (panel c), too, increases stronger with dot 1 present. Only when an electron is added to dot 1, the potential drops discontinuously and the conductance will drop too. At the right-hand side the situation is reversed.

Since the coupling between gate 1 and dot 1 is much stronger than the coupling between gate 1 and dot 2 ($C_{g1} >> C_{12}, C_k$), many electrons are added to the first dot, before one is added to the second, or in other words, in each conductance peak of dot 1, many sawteeth are visible.

5.2 The dot-potential in zero magnetic field

In figure (5.3) the normalized conductances of dot 1 and 2 are shown as a function of scanned gate voltage (V_{g1}); The lower line shows the normal conductance oscillations of a dot in Coulomb blockade, the upper trace is the conductance signal of the voltage-monitoring dot. Very clearly visible are the sawtooth-shaped disturbances due to the adding of single electrons to dot 1. Note that these disturbances line up with the peaks in the conductance of dot 1, as can be expected since transport through a dot is possible when charge degeneracy exists, or in other words, when an electron is added to the dot.

The simulated conductance in figure (5.4) (made by the program in appendix A) shows a good qualitative agreement with the experimental curve in figure (5.3).

The parameters in the figure caption that are marked (*) are obtained by experiment and are certain within about 20 percent. The other parameters are chosen to yield the qualitatively best fit to the curve in figure (5.3). Since there is no geometrical difference between both dots, C_1 and C_2 are defined as being equal. To make contact with the preceding chapter and [3], C_1 and C_2 were made $5*10^{-16}$ F. This yields $\alpha \approx 0.1$. To obtain the right sawtooth-depth, C_k was made $5*10^{-18}$ F, what is reasonable, compared to the other capacities.

In order to obtain the right peak width, after the capacitances were set within their reasonable ranges, the temperature had to be made 0.2 K, although the bulk temperature is only 20 mK. Deviations in this order of magnitude have previously been reported, and 0.2 K is in agreement with the 0.23 K that is reported in [3] for the 'effective line width'. Even when C_1 would be increased by a factor two, and the faults due to the linear approach and experimental uncertainties are also a factor two, an effective electron temperature of about 50 mK would be needed to fit the peak-width. This is still a deviation by a factor 2.5 from the bulk temperature of 20 mK, at which all experiments are done. Although it is possible to obtain even higher electron temperatures at this bulk temperature, due to current heating and the weak electron-phonon interaction at these temperatures [9], current heating is not likely to be the cause of this phenomena in our experiments, since $V_{driving}$ is only $10\mu V$ and the minimum resistance of the dot is about 250 kOhm.
Another explanation for the conductance peak width given in the literature [13?] is an intrinsic broadening of energy levels due to the finite lifetime of single electron states in the dot. An energy level broadening of 100 mK yields via
with $\Gamma = 1/\text{lifetime}$ a single electron state lifetime of 0.08 nanoseconds.

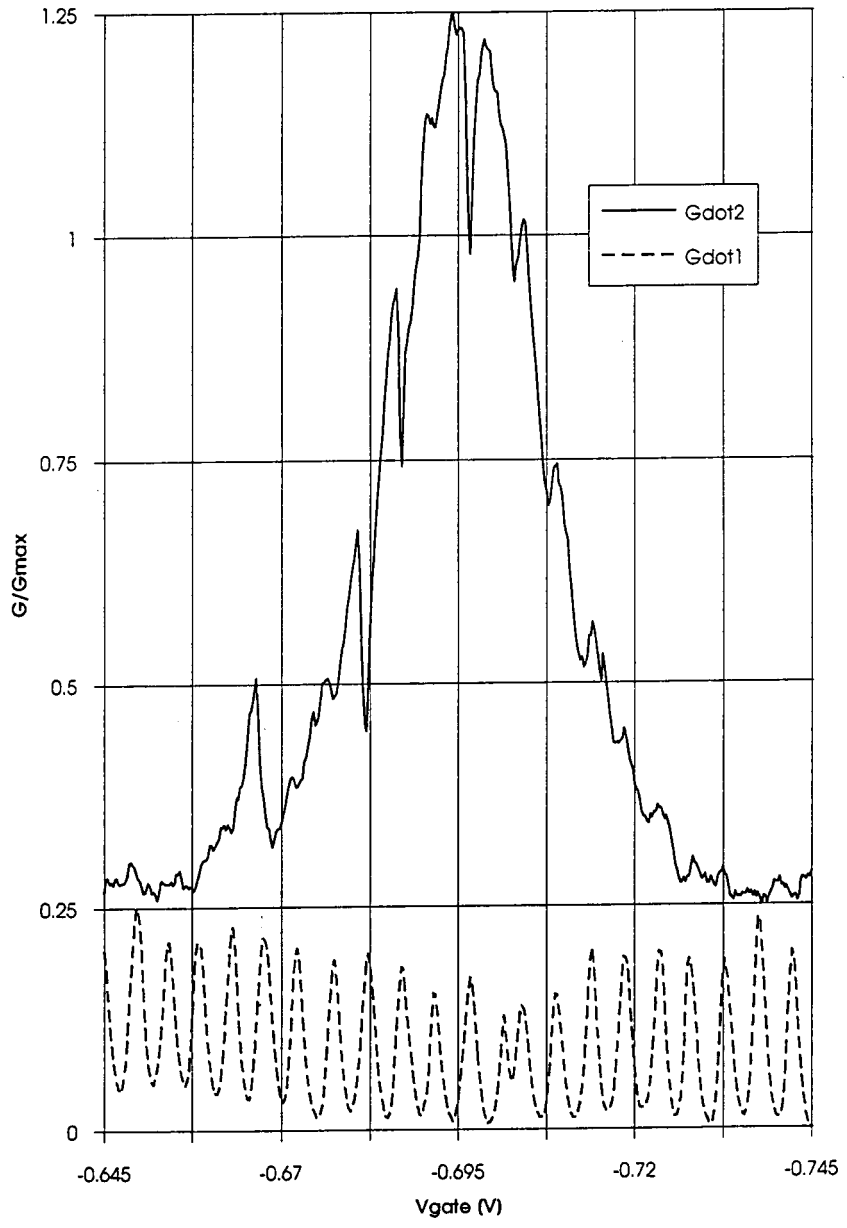

Figure 5.3 Conductance signals of dot 1 and 2, with dot 2 as voltage probe. The traces have been offset for clarity.

$$\hbar\Gamma = k_B T \tag{5.5}$$

Now we have found that a quantum dot can be used as a sensitive voltage probe, two interesting situations can be studied: the transition from one big dot to two smaller dots when the central tunnel barrier is being pinched-off and the transition from an electrically completely isolated dot to a dot that is strongly coupled to the leads.
In the latter experiment the dot that is used as voltage probe, dot 2, is kept unchanged during the whole experiment, i.e. all five enclosing gates are kept at constant voltages. The tunnel barriers that connect the first dot to the leads are adjusted, by changing the bias voltage on the upper and lower left gates, from $R_{pc} \approx 40$kOhm to completely closed. At each tunnelbarrier hight one or more gatescans of V_{g1} were made, see figure (5.5).

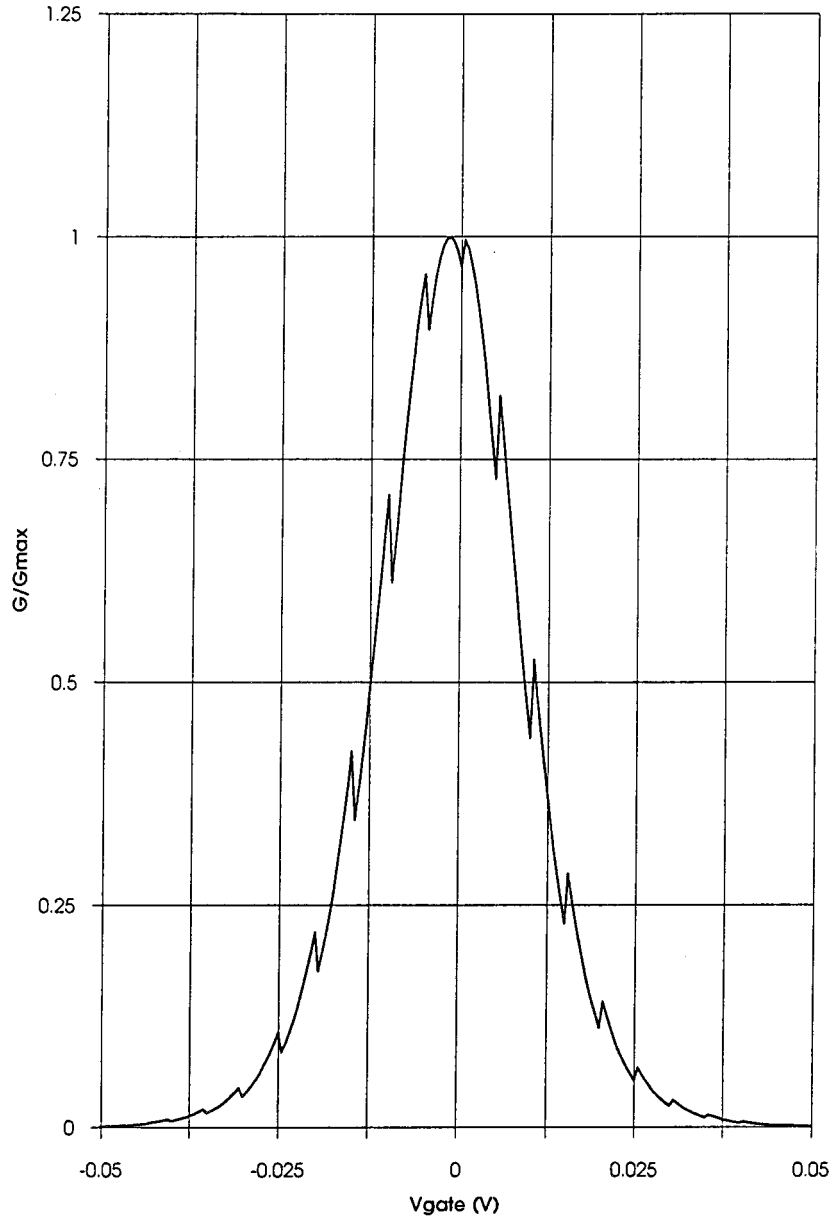

Figure 5.4 Simulated conductance of a dot as voltage probe. The parameters are: $C_1, C_2 = 500$ aF, $C_{g1} = 32$ aF(*), $C_{12} = 1.7$ aF(*), $C_k = 5.0$aF, T=0.2K.

Clearly visible is that the sawtooth oscillations of the potential in dot 1 become weaker when the tunnel barrier hight ($\sim R_{pc}$) is decreased. This can be understood in terms of discreteness of N_1, the number of electrons in dot 1, and tunnelling rate Γ, the rate at which electrons tunnel through a barrier. When the tunnel barrier hight is infinite, Γ becomes zero and N_1 will be the equilibrium number of electrons on the dot, and will not be disturbed by transport through the dot, due to second order processes [10], which causes the number of electrons to vary between N_1 and N_1+1. Since N_1 is sharply defined in this case, also the (electrostatical) potential of dot 1 is fully discrete, and a sharp discontinuity in the potential can be seen when an extra electron is added to the dot.
When the tunnel barrier hight is low, the tunnelling rate increases and N_1 will be less sharply defined since the number of electrons on the dot will be sometimes N_1 and sometimes N_1+1. Thereafter the dot does not fully charge up, and the discontinuities in

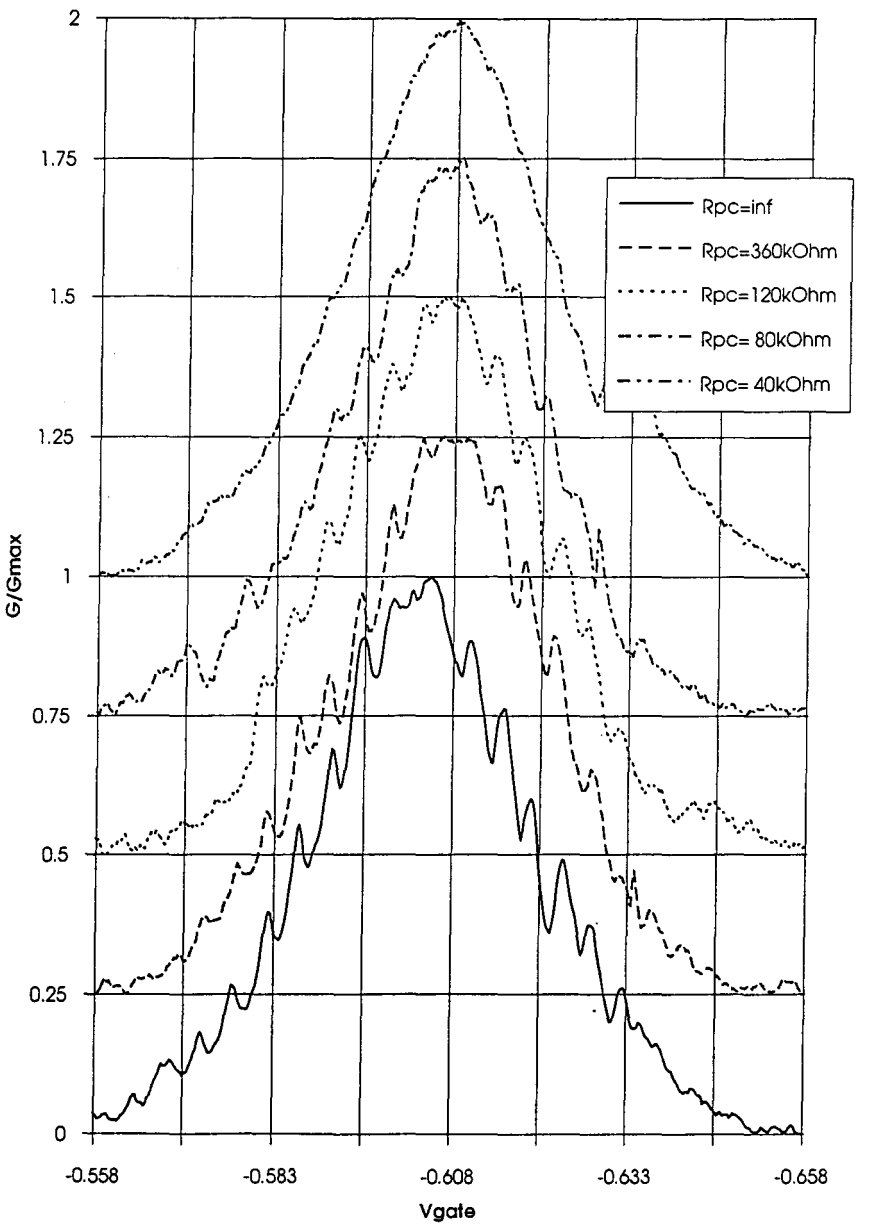

Figure 5.5 Conductance of a dot as voltage probe at different tunnelbarrier hights of the source dot. The tunnelbarrier hight is denoted as an Ohmic resistance R_{pc}.

the potential become smaller and rounded. Both effects are visible in the figure.
During the other experiment, the transition from one to two dots, the bias on the middle two gates was varied, so the conductance of the middle tunnel barrier was adjusted between 0 (at -0.8 V, two separate dots) and 1.5 e^2/h (-0.725 V, one big dot). The other tunnel barriers were adjusted at almost fixed values: the upper and lower left at G=0, the upper and lower right at $\approx$ 1/5 e^2/h.

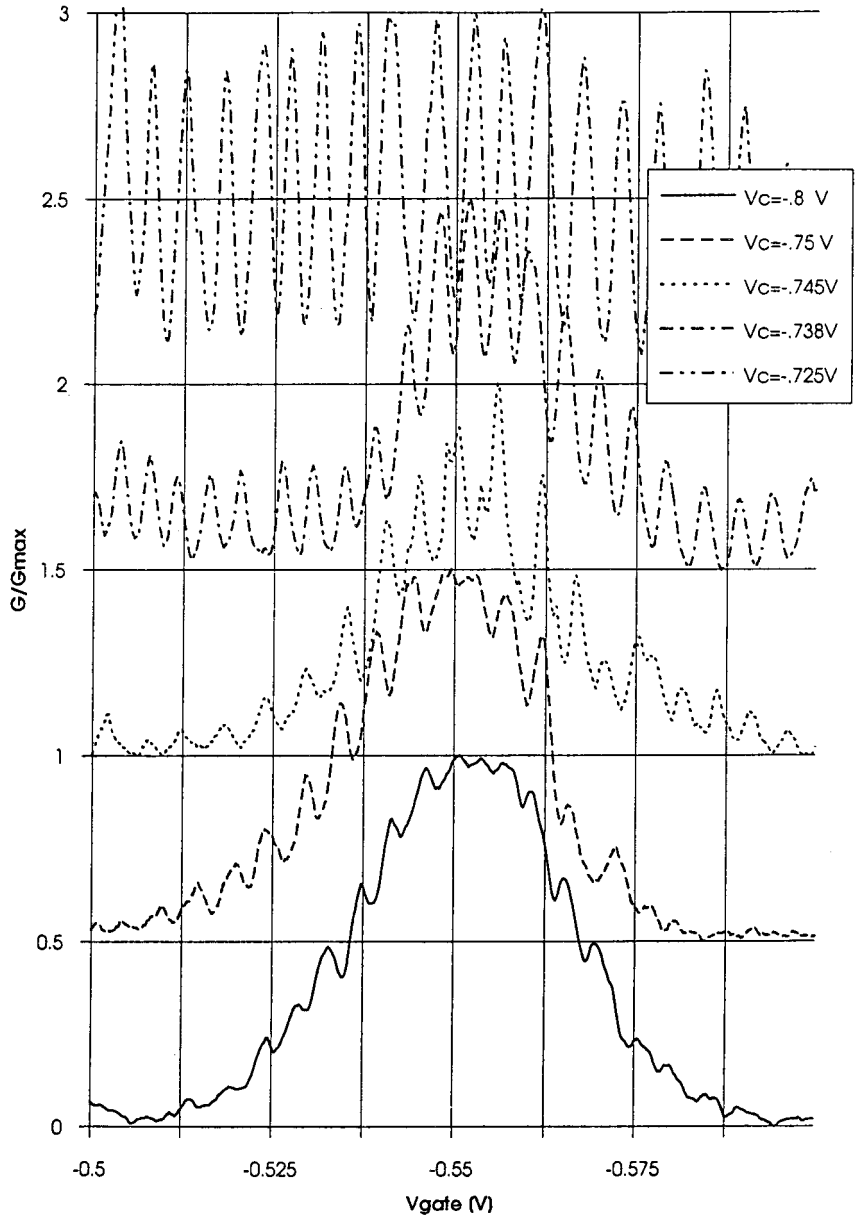

Figure 5.6 Conductance of dot 2 at different hights of the tunnel barrier between both dots, denoted as the voltage on the central gates. Vc=-0.8 corresponds to G=0, Vc=-0.725 to G>e^2/h.

In the lower traces of figure (5.6) the coupling between both dots is seen to increase when the central gates become lower biased, what is probably a result of the decreasing distance between the dots when the separating tunnel barrier is becoming lower and narrower.

The upper traces of the figure show behaviour that is very familiar or even equal to that of a single quantum dot. Note that the period of the oscillations does not change from the lower to the upper trace.

5.3 The potential of a quantum dot in a magnetic field

When a magnetic field is applied to a quantum dot edge states are formed, as described in chapter two. Dependent on how the tunnel barriers are adjusted, the edge states can be localized (figure (5.7)a) or extended (b). The situation with fully localized states corresponds to tunnel barriers with $G < e^2/h$, the situation in panel (b) of the figure corresponds to $e^2/h < G < 2e^2/h$.

The conductance of a quantum dot in these situations can show a more complex structure as a function of gate voltage then in absence of a magnetic field, for example figure (5.8)b, dashed line. The main cause of these phenomena is the cyclical (de)population of Landau levels [11], [16] as the gate voltage is scanned. Cyclical depopulation means that from each Landau level one electron is removed before a second electron is removed from a level.

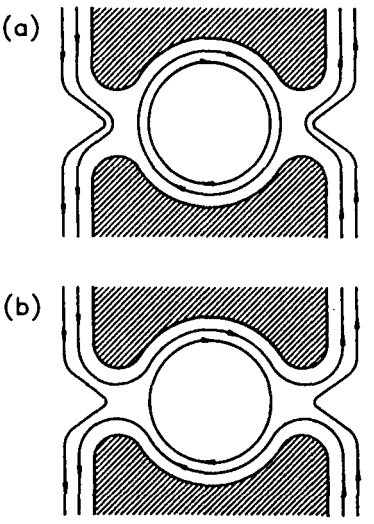

Figure 5.7 Schematic view of a quantum dot with (a) no extended edge chanels, and (b) with one extended and one localized edge chanel.

After the first experimental results [12] on the conductance of quantum dots in the presence of extended edge channels had been reported, the complex conductance signal was sometimes explained as being some sort of Ahronov-Bohm oscillations. When this would be the case, the oscillations should not have any influence on the potential of the dot, since Ahronov-Bohm is caused by electron interference, and does not cause any potential disturbance.

We used a magnetic field of 2.6 Tesla, which yielded four populated Landau levels. Dot 2 was used as voltage probe, with tunnel barriers adjusted at 1/5 e^2/h. The tunnel barriers of the 'source dot', dot 1 were at ½ e^2/h or at 1½ e^2/h, corresponding to zero and one extended edge channel. The conductance traces obtained by scanning V_{gate1} are shown in figure (5.8)a and b respectively. The poor quality of traces, compared to figures (5.6) and (5.7), is due to the fact that another sample had to be used. The dotted line in both figures is the derivative of the conductance of dot 2 with respect to the gate voltage and was numerically obtained. This derivative proved to be a very sensitive tool to see if any periodic modulation, in our case caused by the potential of the source dot, is present on the signal. In figure (5.8)a this is obviously the case, but also in (b) some oscillating behaviour of the derivative with the same period as the finest oscillations on G_{dot1} is visible. We can therefore conclude that all oscillations in the conductance of dot 1 are being caused by potential-influencing processes, i.e. by the removing of electrons, and not by the Ahronov-Bohm effect.

These results can be regarded as the preparation for a new series of experiments on Coulomb blockade in the precence of (partially) transmitted edge channels. Recently, interesting theoretical work has been done by Kinaret *et al.* [15].

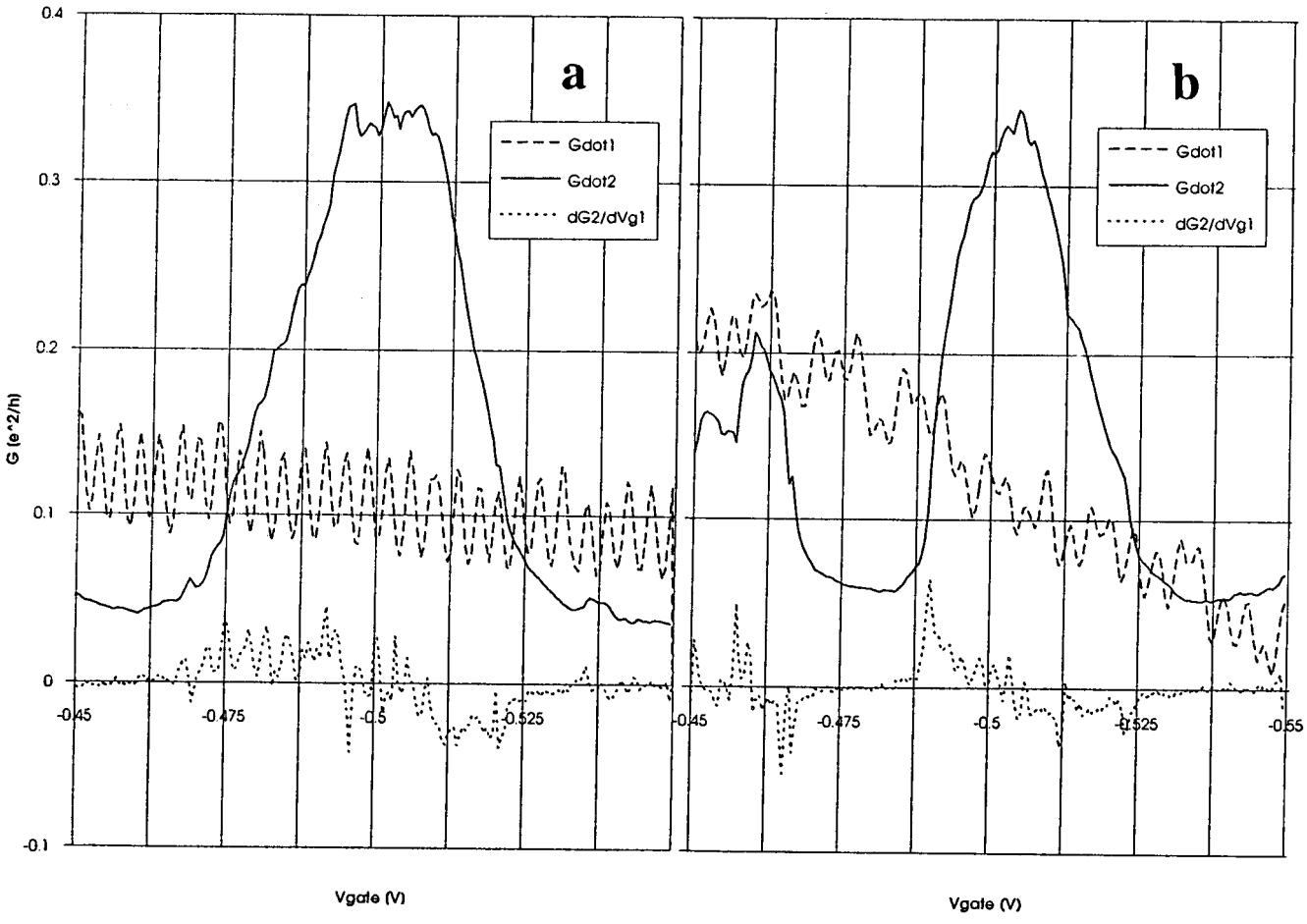

Figure 5.8 Conductance of both dots in presence of (a) zero and (b) one extended edge chanel. dG_2/dV_{g1} in arbitrary units. Gdot1 (b) has been offset $-e^2/h$.

5.4 Conclusion

We have demonstrated that a quantum dot can be used as a very sensitive non-invasive voltage probe for nearby potentials. The influence of these potentials on the conductance of the probe-dot can be described using first order approximations in a slightly modificated version of the standard capacitance model for a single quantum dot.
We used the probe-dot to show that the electrostatical potential of an isolated (high tunnel barriers) quantum dot does vary in a sawtooth-like way as a function of gate voltage. We also found that the measured conductance peak width corresponds to a temperature of about 0.5 K, though the bulk temperature is 20 mK. If this effect is due to electron heating, intrinsic line broadening or even some other effect cannot be concluded from our

experiments.
Finally, we measured the potential of a quantum dot in presence of extended edge channels, and found that the non-standard conductance oscillations of such a system have the same frequency as the modulation of the dot potential, and therefore are probably Coulomb blockade oscillations.

Appendix A

Software

In this section two programs are listed. The first calculates the conductance of a quantum dot when V_{gate} of another nearby dot is scanned, using the formulas of paragraph 5.1. The second counts conductance peaks exceeding a certain hight in a gatescan.

A.1 Program 'Coupling 2 dots'

The program listed below calculates the conductance of a quantum dot that is used as a voltage probe for another nearby quantum dot. The schematic setup for such an experiment is shown in figure (A1).

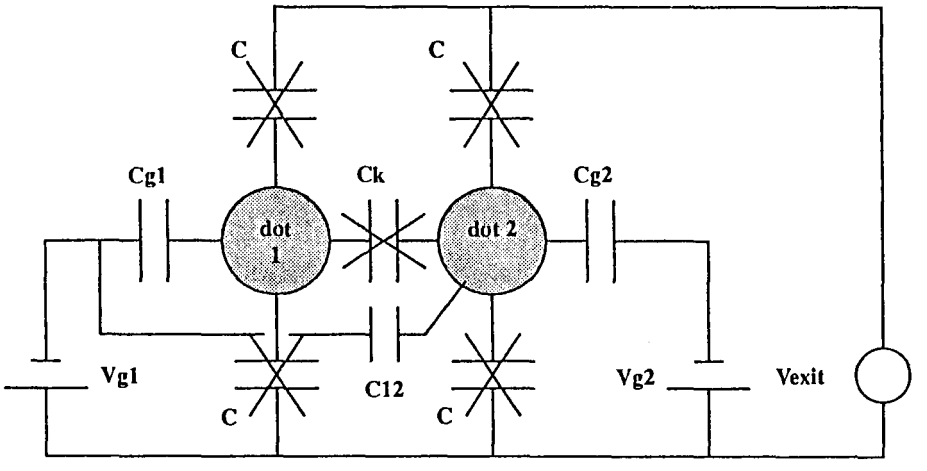

Figure A1 Elecrical equivalent of the double dot sample as used for the simulation of the coupling between two dots

The program steps the gate voltage Vg1 in n_step steps from -Vgrens to +Vgrens and calculates successively the number of electrons on dot 1 (n1), the potential of dot 2 (Vdot2) and the conductance of dot 2 (G). Vg1, Vdot2 and G are stored in the result array G and saved in b:kopsim2.dat as an ASCII-file.
Two remarks have to be made with respect to the program. First, the 'number of electrons' of dot 1, n1, is defined as
which is the deviation from the number of electrons on the dot when Vg1 is zero.

$$n_1 \equiv n_{1,V_{g1}=0} - n_{1,V_{g1}} \tag{A.1}$$

Second, the 'potential of dot 2, ,Vdot2, is in fact the electrochemical potential of the dot, which increases linearly upon Vg1 (at least during one conductance peak) and not the electrostatical potential U, which has a discontinuity at the maximum conductance since the number of electrons changes by one at that point.
The program uses (5.4)

$$\frac{G}{G_{\max}} \approx \cosh^{-2}\left(\frac{Vdot2}{2.5k_BT}\right) \tag{A.2}$$

to calculate the conductance of the dot as a function of Vdot2.
The conductance calculated with the program and parameters as listed below is shown in figure (5.4).

```
program koppeling;
{berekend in een dubbele quantumdot-configuratie de invloed van het scannen
van dot1 m.b.v. Vgate1 op de geleiding G van dot 2. In G staan achtereen-
volgens Vg1, de bijbehorende potentiaal daardoor in dot2-Vdot2 en G.}

const
    C1 = 2.0e-16; {totale capaciteit dot1}
    C2 = 2.0e-16; {tatale capaciteit dot2}
    Cg1 = 3.2e-17; {periode dot1 in Vgate1=e/Cg1}
    Cg2 = 3.3e-17; {periode dot2 in Vgate2=e/Cg2}
    C12= 1.7e-18; {koppeling tussen dot2 en gate1, periode=e/C12}
    Ck = 5.0e-18; {koppeling tussen dot1 en dot2}
    kT = 1.38e-23*0.5; {J}
    e  = 1.6e-19; {Q}
    n_step = 200;
    Vgrens = 0.05; {V. Vg1 loopt van - tot +Vgrens}
    file_out='b:\kopsim2.dat';

var
  G:array [0..n_step,1..3] of real;
  n1, i :integer;
  Vg1, Vdot2, E_red :real;
  f:text;

function cosh(x:real):real;
begin
    cosh:=(exp(x)+exp(-x))/2;
end;
```

```
begin
    n1 := -1*trunc(Vgrens*(Cg1/e));
    for i := 0 to n_step do
    begin
        Vg1 := i*(2*Vgrens/n_step)-Vgrens;
        if Vg1 >= (n1+1)*(e/Cg1) then n1:=n1+1;
        Vdot2:=(C12/C2)*Vg1 + (Ck/C2)*((Cg1/C1)*Vg1 - (e/C1)*n1);
                                {formula (4. )}
        E_red:=(e*Vdot2)/(2.5*kT);
        G[i,3]:=1/sqr(cosh(E_red));
        G[i,1]:=Vg1;
        G[i,2]:=Vdot2;
    end;
    assign (f,file_out);
    rewrite (f);
    for i:=0 to n_step do
    begin
        writeln (f,G[i,1]:8:6,' / ',G[i,2]:8:6,' / ',G[i,3]:8:6);
    end;
    close (f);
end.
```

A.2 Program 'Peakcount'

This program counts the number of conductance peaks that exceed a certain hight. As listed, the program normalizes the conductance such that the minimum conductance is regarded as background and is substracted, and that the remaining maximum conductance is made unity. The results of running this program on the stochastical Coulomb blockade scans at different temperatures, as plotted in figure (4.8), were obtained after the following modification had been made. The -per scan- variable maximum conductance was replaced by an fixed, and for all temperatures equal, maximum conductance, that was regarded as unity.

```
{$M 32768,0,655360}
program peekcnt;

uses crt;

const
    R_ref=120.78; {kOhm}
    e_over_C= 1.6e-19/4.27e-17; {Volt}
    factor=0.5; {mate waarin 2 pieken dichter op elkaar mogen liggen
                 dan op grond van e/C te verwachten is, om nog als af-
                 zonderlijk gedetecteerd te worden}
```

```
    nT_max=30;  {maximum aantal subfile-sets}
    nn_max=8;   {maximum aantal detectie-ondergrenzen!}
    n_col=nn_max+3;{T, G_min, G_max, #_grens(1),..,#_grens(nn_max)}
    data_max=1501; {maximaal aantal meetpunten in een subfile}
type
   a_2D = array [1..nT_max, 1..n_col] of real;
   a_data = array [1..data_max,1..3] of real;
   a_nn = array [0..nn_max] of real;  {let op: a_nn heeft nn_max+1 velden}
   filename = string[79];

var
  file_in, file_out :filename;
  f :text;
  n_sf, n_T, i, ii, n_grens, n_data, of1_of2 :integer;
  result :a_2D;
  x :a_data;
  grens :a_nn;
  dummy :char;


procedure input (var file_in, file_out :filename; var n_grens, n_sf,
        n_T, of1_of2 :integer;var result :a_2D; var grens : a_nn);

var
  j : integer;

begin
    clrscr;
    write('input filename :');
    readln(file_in);
    write('output filename :');
    readln(file_out);
    write('[1] Append of [2] New :');
    readln(of1_of2);
    write('# subfile-sets [bestaande uit x,y,z] :');
    readln(n_T);
    n_sf := n_T*3;
    for j := 1 to n_T do
    begin
       write ('temperatuur horende bij ',j,'e subfile-set [K] :');
       readln (result[j,1]);
    end;
    write('# detectie-ondergrenzen :');
    readln(n_grens);
    grens[0]:=1.001; {nodig voor n_peek procedure}
       writeln('De detectie-ondergrenzen moeten in aflopende volgorde');
       writeln('ingevoerd worden!');
    for j:=1 to n_grens do
```

```
    begin
        write(j,'e detectie-ondergrens [relatief:Gmin=0, Gmax=1] :');
        readln(grens[j]);
    end;
end;

procedure data_in (var f:text; n_data:integer; var x :a_data);
{leest 3 arrays uit file_in in en stopt ze in x. De data file moet reeds ge-
opend zijn. Tussen de data moet alleen een spatie staan. Na elke subfile
moet een <CR> staan.}

var
  j,k :integer;
begin
    for j := 1 to 3 do
    begin
        readln(f);
        for k:=1 to n_data do
        begin
            read(f,x[k,j]);
        end;
    end;
end;

procedure result_out(file_out:filename;n_grens, n_T, of1_of2 :integer;
result:a_2D);
var
  f:text;
  j,k :integer;

begin
    assign(f,file_out);
    if of1_of2=1 then append(f) else
    rewrite(f);
    for j :=1 to n_T do
    begin
        for k :=1 to n_grens+2 do
        begin
            write(f,result[j,k]:8:4);
            write(f,',');
        end;
        write(f,result[j,n_grens+3]:8:4);
        writeln(f);
    end;
    close (f);
end;

procedure G_minmax(x :a_data; n_data,i :integer ;var result:a_2D);
```

```
var
  j :integer;
  G, G_min, G_max :real;

begin
    G_max:=x[1,3]/x[1,2]; G_min:=G_max;
    for j :=1 to n_data do
    begin
        G:= x[j,3]/x[j,2];
        if G>G_max then G_max:=G else
          if G<G_min then G_min:=G;
    end;
    result[i,2]:=G_min; result[i,3]:=G_max;
end;

function G_e2h (G_ratio:real):real;
begin
    G_e2h := G_ratio/R_ref/10*25.812;
end;

function afstand_ok (V1_oud,V2_oud,V1_nieuw,V2_nieuw:real):boolean;
{kijkt of 2 pieken niet veel dichter op elkaar liggen dan op grond van
Cgate te verwachten is.}
var
  afstand :real;
begin
    afstand:=abs(0.5*(V2_oud+V1_oud) - 0.5*(V2_nieuw+V1_nieuw));
    if afstand>factor*e_over_C then afstand_ok:=true
      else afstand_ok:=false;
end;

procedure grenstransform (grens: a_nn; var grens2 :a_nn; result :a_2D;
                          n_grens, i:integer);
var
  j:integer;
begin
    for j:=0 to n_grens do
    begin
        grens2[j]:=result[i,2]+grens[j]*(result[i,3]-result[i,2]);
    end;
end;


procedure n_peek (x:a_data; n_data, n_grens, i:integer; grens:a_nn; var result:
                  a_2D);
{bepaalt het aantal pieken dat boven een bepaalde grens ligt.Het aantal
pieken boven grens(j) = aantal pieken dat eindigt tussen grens(j) en
grens(j-1) + aantal pieken dat boven grens(j-1) eindigt. Dit aantal
```

```
staat in som.}
var
  j,k, som, aantal :integer;
  V1_oud,V2_oud,V1_nieuw,V2_nieuw,G,G_top :real;
  grens2 :a_nn;

begin
    som:=0;
    grenstransform(grens,grens2,result, n_grens, i);
    for j:=1 to n_grens do
    begin
        aantal:=0; k:=1;
        V1_oud:=0;V2_oud:=0;V1_nieuw:=0;V2_nieuw:=0;
        G:=x[1,3]/x[1,2];
        while k<n_data do
        begin
            G_top:=0;
            while (k<n_data) and (G<grens2[j]) do  {zoek begin piek}
            begin
                k:=k+1; G:=x[k,3]/x[k,2];
            end;
            V1_nieuw:=x[k,1];                    {hebbes}
            while (k<n_data) and (G>=grens2[j]) do {zoek einde piek}
            begin
                if G>G_top then G_top:=G;
                k:=k+1; G:=x[k,3]/x[k,2];
            end;
            V2_nieuw:=x[k,1];                    {hebbes}
            if (G_top<grens2[j-1]) and (afstand_ok(V1_oud,V2_oud,V1_nieuw,
            V2_nieuw)) then
            begin  {de piek voldoet aan alle eisen}
                aantal:=aantal+1;
                V1_oud:=V1_nieuw; V2_oud:=V2_nieuw;
            end
            else {de piek is of ruis of al gedetecteerd}
            begin
                if not(afstand_ok(V1_oud,V2_oud,V1_nieuw,V2_nieuw)) then
                begin  {ruis dus}
                    V2_oud:=V2_nieuw; {zo worden door ruis gespleten
                                       pieken als geheel geteld.}
                end
                else   {geen ruis, dus is reeds geteld}
                begin
                    V1_oud:=V1_nieuw; V2_oud:=V2_nieuw;
                    {als de piek geen ruis was, is hij door de vorige
                    grens al gedetecteerd. Hij wordt dan niet geteld
                    maar wel als echt beschouwd.}
                end;
```

```
            end;
        end; {op naar de volgende piek}
        if G_top<grens2[j] then aantal:=aantal-1;
        {kijken of eindpunt niet onterecht als piek is geteld tgv niet
        voldoen aan eis k<n_data}
        som:=som+aantal; result[i,j+3]:=som;
        writeln('grens ',grens[j]:5:3,' aantal: ',aantal:3,' totaal: '
        ,result[i,j+3]:3:0);
    end; {en op naar de volgende grens}
end;



begin
    input(file_in, file_out,n_grens, n_sf,n_T, of1_of2, result, grens);
    assign(f,file_in);
    reset (f);
    write('aantal data in een subfile: ');readln(n_data);
    for i :=1 to n_T do
    begin
{       write('aantal data in 1 subfile voor sf ',(i*3-2),'-',i*3,': ');
        readln (n_data);}{Als niet alle sf zelfde n_data hebben deze invoer
        regel gebruiken, anders bovenstaande}
        data_in(f, n_data,x);
        G_minmax(x, n_data, i, result);
        writeln('subfiles ',i*3-2,'-',i*3,', T=',result[i,1]:5:3,' K');
        writeln('G_min = ',G_e2h(result[i,2]):7:5,' e^2/h');
        writeln('G_max = ',G_e2h(result[i,3]):7:5,' e^2/h');
        n_peek(x, n_data, n_grens, i, grens, result);
    end;
    close (f);
    result_out(file_out, n_grens, n_T, of1_of2, result);
    writeln('druk op een toets om verder te gaan');
    dummy:=readkey;
end.
```

Appendix B

DC-Current amplifier

B.1 Electrical circuit

To be able to do sensitive DC measurements, for example to measure Coulomb staircases, we built a current amplifier based on a design made in Delft University of Technology. Though the group De Mooij is very content with this op-amp design, we were until now unable to do successful measurements with it, probably due to the samples and not to the op-amp.

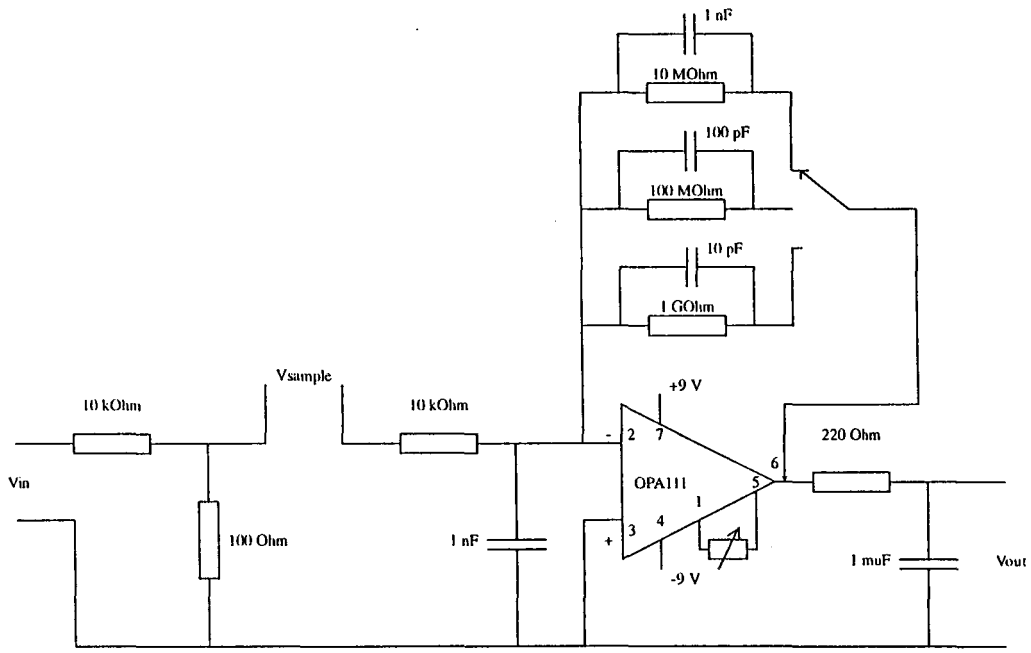

Figure B.1 Electrical circuit of the DC-current amplifier.

The amplifier is very sensitive to AC-signals, for example digital noise from the HP universal source. When used with un-clean driving voltages, a RC filter with a RC time of 0.1 sec or more is strongly advisable.
Another problem of the amplifier is its sensitivity to earth-loops. When switched to 'floating' the complete circuit is disconnected from the grounded case. In this mode of

operation there should always be another grounding-point in the circuit, to prevent sample damage as a result of charging-up of the whole circuit! When switched to 'ground', the circuit is connected to the case. In this mode of operation the inverting input channel of the OPA111 is a (virtual) earth point. All other connections to earth should be avoided in this situation.
Two last tips for operation: Always twist the connecting wires and don't move near the opamp during measurements.

The amplifier is based on the Burr-Brown OPA111AM operational amplifier. The amplification factor is given by the general op-amp relation

$$V_{uit} = R * I_{sample}$$

where R is the resistance between the output and inverting input channel and I_{sample} the current through the sample. For our op-amp this gives amplification factors of 10^7 to 10^9. The capacitances parallel to these resistances are used to filter out AC signals.
Directly behind the driving voltage input a divider (factor 100) is placed, to make the use of non-precision voltage sources possible.

Acknowledgement

The past ten months I have worked with great pleasure on the Coulomb blockade experiments, not in the last place because of the people I worked with. On this place I want to thank everyone who helped me in whatever way.
In the first place I want to thank Laurens Molenkamp for his excellent guidance and his stimulating enthusiasm for ongoing and future experiments. Furthermore, I'd like to thank Menno Mabesoone for teaching me how to operate the dilution refrigerator and continuous technical assistance.
I owe thanks to Prof. Dr. J.H. Wolter for giving me the opportunity to have the valuable experience of working on the Philips Nat. Lab.
Other people I certainly want to thank are Paul Blom, Hans Buyk, Sander den Hartog, Henk van Houten, Marc de Jong, Eric-Jan Lous, Ad Nagelkerke, Toine Staring, Nijs van der Vaart and Fred de Wit.
Finally I want to thank Marco Brugmans for bringing me in contact with Laurens Molenkamp.

Bibliography

[1] C.J. Gorter, Physica **17**, 777 (1951)

[2] T. A. Fulton and G. J. Dolan, Phys. Rev. Lett. **59**, 109 (1987)

[3] A. A. M. Staring, Ph.D. Thesis Eindhoven University of Technology (1992)

[4] L. P. Kouwenhoven, Ph.D. Thesis Delft University of Technology (1992)

[5] K. K. Likharev, I.B.M. J. Res. Dev. **42**, 144 (1988); D. V. Averin and K. K. Likharev in: 'Mesoscopic Phenomena in Solids', edited by B. L. Al'tshuler, P. A. Lee and R. A. Webb (Elsevier, Amsterdam, 1991) p. 167

[6] L. I. Glazman and V. Chandrsekhar, Europhys. Lett. **19** (7) 623 (1992)

[7] I. M. Ruzin, V. Chandrasekhar, E. I. Levin and L. I. Glazman, Phys. Rev. B. **45** (23) 13469 (1992)

[8] M. Field, C. G. Smith et al., Phys. Rev. Lett. **70**, (9) 1311 (1993)

[9] L. W. Molenkamp, H. van Houten, C. W. J. Beenakker, R. Eppenga and C. T. Foxon in: 'Condensed Systems of Low Dimensionality', edited by J. L. Beeby et al. (Plenum Press, New York, 1991) p. 335

[10] D. V. Averin and Yu. V. Nazarov, Macroscopic Quantum Tunneling of Electric Charge and Co-tunneling in Systems of Small Tunnel Junctions, to be published.

[11] A. A. M. Staring, B. W. Alphenaar, H. van Houten, L. W. Molenkamp, O. J. A. Buyk, M. A. A. Maabesoone and C. T. Foxon, Phys. Rev. B **46**, 12869 (1992)

[12] B. W. Alphenaar, A. A. M. Staring, H. van Houten, O. J. A. Buyk, M. A. A. Mabesoone and C. T. Foxon, Phys. Rev. B **46**, 7236 (1992)

[13] C. W. J. Beenakker, Phys. Rev. B **44**, 1646 (1991)

[14] F. M. de Aguiar and D. A. Wharam, Phys. Rev. B. **43**, 9984 (1991)

[15] J. M. Kinaret and N. S. Wingreen, to be published.

[16] I. K. Marmorkos and C. W. J. Beenakker, Phys. Res. B **46**, 15562 (1992)

[17] U. Sivan, F. P. Milliken, K. Milkove, S. Rishton, Y. Lee, J. M. Hong, V. Boegli, D. Kern, M. deFranza, to be published.